


1-31-1991

Investigations of substitution of Bi and Tl for rare earth elements in superconducting $\text{RBa}_2\text{Cu}_3\text{O}_y$

Jian Tang
New Jersey Institute of Technology

Follow this and additional works at: <https://digitalcommons.njit.edu/theses>

 Part of the [Chemistry Commons](#)

Recommended Citation

Tang, Jian, "Investigations of substitution of Bi and Tl for rare earth elements in superconducting $\text{RBa}_2\text{Cu}_3\text{O}_y$ " (1991). *Theses*. 1881.
<https://digitalcommons.njit.edu/theses/1881>

This Thesis is brought to you for free and open access by the Electronic Theses and Dissertations at Digital Commons @ NJIT. It has been accepted for inclusion in Theses by an authorized administrator of Digital Commons @ NJIT. For more information, please contact digitalcommons@njit.edu.

Copyright Warning & Restrictions

The copyright law of the United States (Title 17, United States Code) governs the making of photocopies or other reproductions of copyrighted material.

Under certain conditions specified in the law, libraries and archives are authorized to furnish a photocopy or other reproduction. One of these specified conditions is that the photocopy or reproduction is not to be “used for any purpose other than private study, scholarship, or research.” If a user makes a request for, or later uses, a photocopy or reproduction for purposes in excess of “fair use” that user may be liable for copyright infringement,

This institution reserves the right to refuse to accept a copying order if, in its judgment, fulfillment of the order would involve violation of copyright law.

Please Note: The author retains the copyright while the New Jersey Institute of Technology reserves the right to distribute this thesis or dissertation

Printing note: If you do not wish to print this page, then select “Pages from: first page # to: last page #” on the print dialog screen

The Van Houten library has removed some of the personal information and all signatures from the approval page and biographical sketches of theses and dissertations in order to protect the identity of NJIT graduates and faculty.

ABSTRACT

Title of Thesis:

Investigations of Substitution of Bi and Tl for Rare
Earth Elements in Superconducting $\text{RBa}_2\text{Cu}_3\text{O}_y$
Jian Tang, Master of Science, 1991

Thesis directed by:

Professor Lawrence Suchow

Substitution of some other elements for rare earth or yttrium in high- T_c superconducting $\text{RBa}_2\text{Cu}_3\text{O}_y$ compounds ($R = \text{Y, Nd, etc.}$) may improve chemical and physical properties of the materials, shed light on the superconducting mechanism of the new materials, and help to find new superconducting materials with even higher transition temperatures.

Bi^{3+} and Tl^{3+} have been reported earlier to result in higher T_c 's in the related layer-structure compounds. The effect of electronegativity on superconductivity could be studied if substitution of Bi or Tl for Y or other rare earth elements in $\text{RBa}_2\text{Cu}_3\text{O}_y$ could be realized.

Earlier researchers have indicated that, under oxidizing conditions at the reaction temperature (about 900°C), Bi^{3+} does not enter $\text{YBa}_2\text{Cu}_3\text{O}_y$ but that a non-superconducting perovskite phase Ba_2BiYO_6 (with Bi^{5+}) is formed instead. In the present work, attempts have been made to prepare superconducting $(\text{R,Bi})\text{Ba}_2\text{Cu}_3\text{O}_y$ by first forming the non-superconducting, oxygen-deficient, tetragonal form in an inert atmosphere and then introducing additional oxygen and converting to the orthorhombic form by reheating in air or

oxygen at lower temperature (about 250 - 500°C). X-ray diffraction, optical microscopy, thermogravimetric analysis, and electrical measurements were used to study the reaction products.

It was found that, in an inert atmosphere, $\text{YBa}_2\text{Cu}_3\text{O}_y$ is very difficult to form while Ba_2BiYO_6 , a non-superconducting phase, still forms as it does under oxidizing conditions, with oxidation of Bi^{3+} to Bi^{5+} probably due to reduction of Cu^{2+} to Cu^+ ; $(\text{Y,Bi})\text{Ba}_2\text{Cu}_3\text{O}_y$ is not formed.

In an oxidizing atmosphere, both $\text{NdBa}_2\text{Cu}_3\text{O}_y$ and $\text{Ba}_2\text{BiNdO}_6$ with a structure similar to that of Ba_2BiYO_6 result; there is no evidence for the formation of $(\text{Nd,Bi})\text{Ba}_2\text{Cu}_3\text{O}_y$ to any significant degree. The presence of $\text{Ba}_2\text{BiNdO}_6$, a minority and insulating phase, along with $\text{NdBa}_2\text{Cu}_3\text{O}_y$ results in a broader transition temperature and an increase in normal state resistivity.

In an inert atmosphere, the formation of both $\text{NdBa}_2\text{Cu}_3\text{O}_y$ and $\text{Ba}_2\text{BiNdO}_6$ is hindered and a tetragonal $\text{NdBa}_2\text{Cu}_3\text{O}_y$ and poorly crystallized and probably oxygen-deficient $\text{Ba}_2\text{BiNdO}_x$ result. Superconductivity of the samples with Bi addition is severely deteriorated since the tetragonal $\text{NdBa}_2\text{Cu}_3\text{O}_y$ is not easily converted to an optimum orthorhombic structure while the insulating $\text{Ba}_2\text{BiNdO}_6$ appears in the samples during the after-annealing.

Tl was found not to enter the Y sites of $\text{YBa}_2\text{Cu}_3\text{O}_y$ under oxidizing conditions.

**Investigations of Substitution of Bi and Tl for Rare
Earth Elements in Superconducting $\text{RBa}_2\text{Cu}_3\text{O}_y$**

by

Jian Tang

Thesis submitted to the Faculty of the Graduate School of
the New Jersey Institute of Technology in partial
fulfillment of the requirements for the degree of
Master of Science in Applied Chemistry
1991

APPROVAL SHEET

Title of Thesis: Investigations of Substitution of Bi and Tl
for Rare Earth Elements in Superconducting
 $\text{RBa}_2\text{Cu}_3\text{O}_y$

Name of Candidate: Jian Tang

Thesis and Abstract Approved:

Dr. Lawrence Suchow
Professor of Chemistry

Date

Dr. Reginald P.T. Tomkins
Professor of Chemistry

Date

Dr. Barbara Kebbekus
Professor of Chemistry

Date

VITA

Name: Jian Tang

Permanent address: Department of Materials Science and Engineering, Wuhan University of Technology, Wuhan, Hubei Province, People's Republic of China

Degree and date to be conferred: Master of Science in Applied Chemistry, 1991

Date of birth:

Place of birth:

Secondary education: The high school attached to the Normal University of Southwest China, 1974

Collegiate institutions attended	Date	Degree/Date
Wuhan University of Technology	2/78-1/82	B.S., 1982
Wuhan University of Technology	2/82-12/84	M.S., 1985
New Jersey Institute of Technology	9/88-10/90	M.S., 1991

Major: Applied Chemistry

Minor: Materials Science and Engineering

Publications: The Influence of Phase Separation on T_g of Glasses, J. Wuhan University of Technology, 1(2), 64(1986).

Positions held: Lecturer, Department of Materials Science and Engineering, Wuhan University of Technology, Wuhan, Hubei Province, P.R.China.

ACKNOWLEDGMENTS

I wish to thank my thesis advisor, Dr. Lawrence Suchow, who has patiently guided me through this research and financially helped me to complete my education here at NJIT. I am also grateful to Dr. Steven Sunshine of AT&T Bell Laboratories for making his apparatus available to me for electrical measurement. I wish also to express my appreciation to Dr. Su-ling Cheng and Mr. Zhen-di Tong, who helped me in thermogravimetric analysis with their equipments at the Advanced Technology Center of NJIT.

Finally, I owe many thanks to my patient wife, Yanping.

Jian Tang

CONTENTS

	I. INTRODUCTION	1
	I.1. Superconductivity: Materials And Theory	1
	I.2. A Review of New Oxide Superconductors	7
	I.2.1. La_2CuO_4 -based Compounds	7
H	I.2.2. YBa Cu O and $\text{LnBa}_2\text{Cu O}$ Compounds	8
	I.2.3. Bismuth and Thallium Copper Oxides	10
	I.2.4. Some Other Superconducting Oxides	10
	I.3. Perovskite Structure and Superconductivity	14
	I.3.1. Perovskite Structure and Ba(Pb,Bi)O_3 Superconductor	14
	I.3.2. $(\text{Ba,K})\text{BiO}_3$ Superconductor	18
	I.4. $\text{YBa}_2\text{Cu}_3\text{O}_y$ Structures, Structure Transitions and Substitutions	19
	I.4.1. $\text{YBa}_2\text{Cu}_3\text{O}_y$ Structures	19
	I.4.2. Orthorhombic-Tetragonal Transition in $\text{RBa}_2\text{Cu}_3\text{O}_y$	21
	I.4.3. Substitutions in $\text{YBa}_2\text{Cu}_3\text{O}_y$	28
	I.4.3.1. Copper substitution effects: $\text{YBa}_2(\text{Cu}_{1-x}\text{M}_x)_3\text{O}_y$	28
	I.4.3.2. Barium substitution effects	32
	I.4.3.3. Substitution for Y in $\text{YBa}_2\text{Cu}_3\text{O}_y$	32
	I.5. Substitution of Bi for Y: Questions and Significance	35
	I.5.1. Substitution of Bi for Y: A Possibility	35
	I.5.2. Substitution of Bi for Y: Significance	40
	II. EXPERIMENTS	46
	II.1. Sample Preparations	46
	II.2. X-Ray Diffraction Investigations	49
	II.3. Microscopy	50
	II.4. Thermogravimetric Analysis (TGA)	50
	II.5. Electrical Measurements	51
	III. RESULTS AND DISCUSSION	51
	III.1. $\text{Y}_{1-x}\text{Bi}_x\text{Ba}_2\text{Cu}_3\text{O}_y$ System	51
	III.2. $\text{Nd}_{1-x}\text{Bi}_x\text{Ba}_2\text{Cu}_3\text{O}_y$ System	54
	III.2.1. Preparations in Air	54
	III.2.2. Preparations in Inert Atmosphere	60
	III.2.2.1. Reactions in inert atmosphere	60
	III.2.2.2. Annealing to reintroduce oxygen	66
	III.2.2.3. Where are the Bi ions?	68
	III.2.3. Preparations in Reducing Atmosphere	81
	III.3. Some Other Systems	81
	III.3.1. $\text{Y}_{1-x}\text{Tl}_x\text{Ba}_2\text{Cu}_3\text{O}_y$	81
	III.3.2. $\text{La}_{1-x}\text{Bi}_x\text{Ba}_2\text{Cu}_3\text{O}_y$	81
	IV. CONCLUSIONS	82
	REFERENCES	84
	APPENDIX I	92
	APPENDIX II	100

List of Tables

1 Superconductivity parameters of the elements	3
2 Superconductivity of selected compounds	4
3 $(AO)_m M_2 Ca_{n-1} Cu_n O_{2n+2}$ phases	11
4 T_C 's and structures for low- T_C superconducting oxides	16
5 Effective ionic radii of selected ions	39
6 Electronegativity of selected elements	45
7 Melting points of selected compounds	48
8 X-ray phase analysis in the $Y_{1-x} Bi_x Ba_2 Cu_3 O_y$ system	52
9 X-ray phase analysis for $Nd_{1-x} Bi_x Ba_2 Cu_3 O_y$ prepared in air	55
10 Superconducting transition temperatures for nominal $Nd_{1-x} Bi_x Ba_2 Cu_3 O_y$ compounds	58
11 X-ray phase analysis for $Nd_{1-x} Bi_x Ba_2 Cu_3 O_y$ prepared in N_2	61
12 X-ray phase analysis for $Nd Ba_2 Cu_{3-z} Bi_z O_y$ and $Nd_{1-x} Bi_x Ba_2 Cu_{2.9} Bi_{0.1} O_y$ prepared in N_2	65
13 X-ray phase analysis for products of reaction between Nd-123 and excess $Bi_2 O_3$	70
14 Temperatures of TGA onset and maximum weight increase of the samples made in N_2	73

List of Figures

1 a. Resistance in ohms of a specimen of mercury vs. absolute temperature	2
b. Meissner effect in a superconducting sphere cooled in a constant applied magnetic field	2
2 Structure of the "single-layered" $\text{La}_{2-x}\text{R}_x\text{CuO}_4$ compound	9
3 Structure of the "multilayered" $\text{Tl}_m\text{Ca}_{n-1}\text{Ba}_2\text{Cu}_n\text{O}_{2n+m+2}$ or $\text{Bi}_m\text{Ca}_{n-1}\text{Sr}_2\text{Cu}_n\text{O}_{2n+m+2}$ compounds	12
4 Members of the family $\text{Pb}_2\text{M}_2\text{M}'_{n-1}\text{Cu}_{n+1}\text{O}_{4+2n+x}$	13
5 The primitive cubic unit cell of a perovskite compound ABO_3	15
6 Crystal structure of several members of the $\text{Ba}_{1-x}\text{K}_x\text{BiO}_3$ series	15
7 Structure of "double-layered" $\text{YBa}_2\text{Cu}_3\text{O}_y$	20
8 Thermogravimetric analysis (TGA) trace for a $\text{YBa}_2\text{Cu}_3\text{O}_y$ sample	23
9 Effect of processing treatments on the resistivity- temperature dependence of an $\text{ErBa}_2\text{Cu}_3\text{O}_y$ sample	24
10 Effect of changing the oxygen content on the properties of $\text{YBa}_2\text{Cu}_3\text{O}_y$	24
11 Effect of processing heat treatments on the superconducting properties of $\text{YBa}_2\text{Cu}_3\text{O}_y$	27
12 Superconducting transition temperature vs. dopant concentration for $\text{YBa}_2(\text{Cu}_{1-x}\text{M}_x)_3\text{O}_y$	29

13	Schematic diagram for high temperature processing of $\text{LaBa}_2\text{Cu}_3\text{O}_y$ with T_C ($R=0$) above 90 K	34
14	Structure of Ba_2BiYO_6	37
15	T_C as a function of for some high-temperature superconductors	42
16	T_C as a function of electronegativity difference for some oxide high- T_C superconductors	44
17	Electrical resistance vs. temperature for nominal $\text{Nd}_{1-x}\text{Bi}_x\text{Ba}_2\text{Cu}_3\text{O}_y$ prepared in air	57
18	Electrical resistance vs. temperature for nominal $\text{Nd}_{1-x}\text{Bi}_x\text{Ba}_2\text{Cu}_3\text{O}_y$ prepared in N_2	67
19	TGA results for nominal $\text{Nd}_{1-x}\text{Bi}_x\text{Ba}_2\text{Cu}_3\text{O}_y$ samples	72

I. INTRODUCTION

I.1. Superconductivity: Materials And Theory

It has long been known that the electrical resistivity of many metals and alloys suddenly drops to zero when the specimen is cooled to sufficiently low temperature, often a temperature in the liquid helium range. This phenomenon, called superconductivity, was observed first by Kamerlingh Onnes^[1] in a specimen of mercury in 1911, three years after he first liquefied helium. At a critical temperature (T_C) the specimen undergoes a phase transition from a state of normal electrical resistivity to a superconducting state (Fig.1a). At the same time, if the specimen is placed in a magnetic field, the magnetic flux originally present is ejected from the specimen. This is called the Meissner effect (Fig.1b) which is central to the characterization of the superconducting state and cannot be accounted for by the assumption that a superconductor is a normal conductor with zero electrical resistivity.^[2]

It has since been found that superconductivity occurs in many metallic elements of the periodic system and also in alloys, intermetallic compounds, and doped semiconductors (Tables 1 and 2). The range of transition temperatures (for these materials) known at present extends from 23.2 K for the compound Nb_3Ge to below 0.001 K for the element Rh. Several materials become superconducting only under high

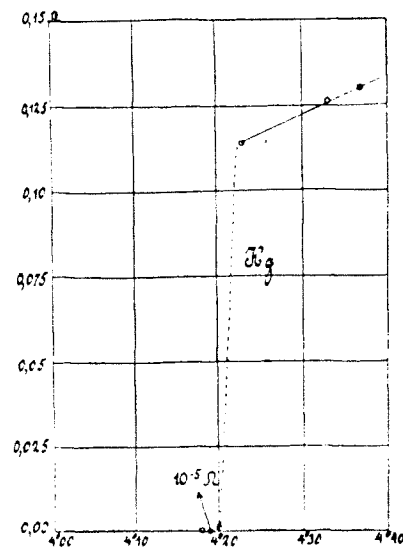


Figure 1a. Resistance in ohms of a specimen of mercury versus absolute temperature. This plot by Kamerlingh Onnes marked the discovery of superconductivity.[1]

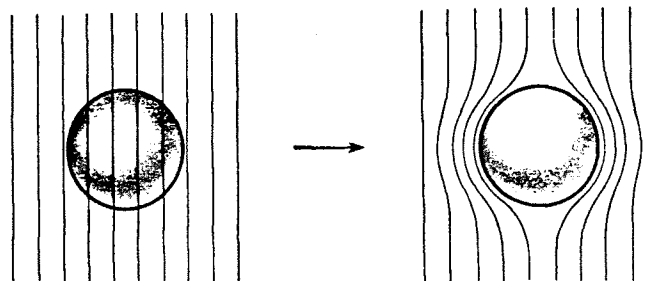


Figure 1b. Meissner effect in a superconducting sphere cooled in a constant applied magnetic field; on passing below the transition temperature the lines of induction B are ejected from the sphere.[2]

Table 1 Superconductivity parameters of the elements												B	C	N	O	F	Ne																												
Li	Be 0.026	An asterisk denotes an element superconducting only in thin films or under high pressure in a crystal modification not normally stable. [2]										Al	Si*	P*	S*	Cl	Ar																												
Na	Mg											1.140 105																																	
Transition temperature in K																																													
Critical magnetic field at absolute zero in gauss (10 ⁻⁴ tesla)																																													
K	Ca	Sc	Ti 0.39 100	V 5.39 1420	Cr*	Mn	Fe	Co	Ni	Cu	Zn 0.875 53	Ga 1.091 51	Ge*	As*	Se*	Br	Kr																												
Rb	Sr	Y*	Zr 0.546 47	Nb 9.50 1980	Mo 0.92 95	Tc 7.77 1410	Ru 0.51 70	Rh 0.003 049	Pd	Ag	Cd 0.56 30	In 3.4035 293	Sn _(w) 3.722 309	Sb*	Te*	I	Xe																												
Cs*	Ba*	La _{fcc}	Hf 0.12 1100	Ta 4.45 830	W 0.012 1.07	Re 1.4 198	Os 0.655 65	Ir 0.14 19	Pt	Au	Hg _(n) 4.153 412	Tl 2.39 171	Pb 7.193 803	Bi*	Po	At	Rn																												
Fr	Ra	Ac	<table><tr><td>Ce*</td><td>Pr</td><td>Nd</td><td>Pm</td><td>Sm</td><td>Eu</td><td>Gd</td><td>Tb</td><td>Dy</td><td>Ho</td><td>Er</td><td>Tm</td><td>Yb</td><td>Lu 0.1</td></tr><tr><td>Th 1.759 1.62</td><td>Pa 1.4</td><td>U*(α)</td><td>Np</td><td>Pu</td><td>Am</td><td>Cm</td><td>Bk</td><td>Cf</td><td>Es</td><td>Fm</td><td>Md</td><td>No</td><td>Lr</td></tr></table>															Ce*	Pr	Nd	Pm	Sm	Eu	Gd	Tb	Dy	Ho	Er	Tm	Yb	Lu 0.1	Th 1.759 1.62	Pa 1.4	U*(α)	Np	Pu	Am	Cm	Bk	Cf	Es	Fm	Md	No	Lr
Ce*	Pr	Nd	Pm	Sm	Eu	Gd	Tb	Dy	Ho	Er	Tm	Yb	Lu 0.1																																
Th 1.759 1.62	Pa 1.4	U*(α)	Np	Pu	Am	Cm	Bk	Cf	Es	Fm	Md	No	Lr																																

Table 2. Superconductivity of selected compounds^[2]

Compound	T _C (K)	Compound	T _C (K)
Nb ₃ Ge	23.2	V ₃ Si	17.1
Nb ₃ Sn	18.05	V ₃ Ga	16.5
Nb ₃ Al	17.5	Pb ₁ Mo _{5.1} S ₆	14.4
NbN	16.0	La ₃ In	10.4
(SN) _x polymer	0.26	Ti ₂ Co	3.44

pressure; for example, Si has a superconducting form at 165 kbar, with $T_C = 8.3$ K. It was also found that, in experimental searches for superconductors with ultralow transition temperatures it is important to eliminate from the specimen even trace quantities of foreign paramagnetic elements because they can lower the transition temperature severely. One part of Fe in 10^4 will destroy the superconductivity of Mo, which when pure has $T_C = 0.92$ K; and 1 atom percent of gadolinium lowers the transition temperature of lanthanum from 5.6 to 0.6 K. Nonmagnetic impurities have little effect on the transition temperature.

The basis of a quantum theory of superconductivity of the old type of superconductors (a new type of superconducting materials, oxides, will be reviewed in detail later) was laid by the classic 1957 papers of Bardeen, Cooper, and Schrieffer (BCS).^[3] The accomplishments of the BCS theory include:^[2]

1. An attractive interaction between electrons can lead to a ground state separated from excited states by an energy gap. Critical magnetic field (to destroy the superconductivity), thermal properties, and most of electromagnetic properties are consequences of the energy gap.

2. The electron-lattice-electron interaction leads to an energy gap of the observed magnitude. The indirect interaction proceeds when one electron interacts with the lattice and deforms it; a second electron sees the deformed lattice

and adjusts itself to take advantage of the deformation to lower its energy. Thus the second electron interacts with the first electron via the lattice deformation.

3. The criterion for the transition temperature of an element or alloy involves the electron density of orbitals $D(\epsilon_F)$ of one spin at the Fermi level and the electron-lattice interaction U , which can be estimated from the electrical resistivity because the resistivity at room temperature is a measure of the electron-phonon interaction. For $UD(\epsilon_F) \ll 1$ the BCS theory predicts

$$T_C = 1.14\theta \exp[-1/UD(\epsilon_F)]$$

where θ is the Debye temperature and U is an attractive interaction. The result for T_C is satisfied at least qualitatively by the experimental data. There is an interesting apparent paradox: the higher the resistivity at room temperature the higher is U , and thus the more likely it is that a metal will be a superconductor when cooled.

All in all, the BCS theory accounts for a superconducting state formed from pairs of electrons which are called Cooper pairs. However, since 1986 the BCS theory has been facing a big challenge due to the discovery of new types of superconductors, oxide high- T_C superconducting materials which cannot be entirely explained by the simple free-electron picture.

I.2. A Review of New Oxide Superconductors

Based on a large amount of experimental information and theoretical understanding, the prevailing view prior to 1986, when high-temperature superconductivity in oxides was discovered, was that the maximum value of the superconducting transition temperature T_C of any materials would not increase much above about 23 K, the high T_C record held since 1973 by the A15 compound Nb_3Ge . In fact, between 1911 and 1986, T_C only increased at an average rate of about 0.25 K per year. However, between 1986 and 1989 the maximum T_C value of the new copper oxide superconductors rose at an average rate of about 30 K per year to its present value of about 122 K. Thus, superconductivity near or above room temperature no longer seems out of the question, as it did a few short years ago. Moreover, the oxides were generally regarded as the least likely candidates for high T_C superconductivity due to their low concentrations of charge carriers. An understanding of the origin and nature of high T_C superconductivity in the new oxide compounds constitutes one of the most important and challenging scientific problems that has emerged in recent years.

I.2.1. La_2CuO_4 -based compounds

In 1986, Bednorz and Müller [4] discovered that a copper oxide-based material, $La_{2-x}Ba_xCuO_{4-y}$, is responsible for the indications of superconductivity at about 30 K. Since then,

many new high- T_C superconducting oxide materials have been discovered.

The structure of $\text{La}_{2-x}\text{Ba}_x\text{CuO}_{4-y}$ is identical to that of the undoped orthorhombic La_2CuO_4 structure or its high-temperature tetragonal polymorph which belongs to a K_2NiF_4 structure (Fig.2) It can be described either as a stacking of perovskite and NaCl cubes or as a layered compound. The oxygen-defect perovskite La_2CuO_4 is semiconducting, but by replacing some of the trivalent La by divalent Ba, Ca and Sr, some of the Cu^{2+} in the compound is oxidized to Cu^{3+} to give a mixed valence ($\text{Cu}^{2+}/\text{Cu}^{3+}$) compound. The orthorhombicity of the La_2CuO_4 is decreased and superconducting compounds are produced.[5] A maximum superconducting transition, $T_C = 40$ K, is obtained at $x = 0.15$ in $\text{La}_{2-x}\text{Sr}_x\text{CuO}_{4-y}$.

I.2.2. $\text{YBa}_2\text{Cu}_3\text{O}_y$ and $\text{LnBa}_2\text{Cu}_3\text{O}_y$ compounds

The discovery of superconductivity at 90 K in a material now known to have the chemical formula $\text{YBa}_2\text{Cu}_3\text{O}_y$, where $y > 6.8$, gave a great impetus to the field of high- T_C superconductivity in oxides, since it broke the 77 K liquid nitrogen temperature barrier.[6] Shortly thereafter, superconductivity with $T_C = 90-94$ K was discovered in the lanthanide analogues $\text{LnBa}_2\text{Cu}_3\text{O}_y$ where Ln is a lanthanide element except for Ce, Pr, Pm, and Tb.[7] Because the studies in this thesis deal with substitutions for the rare earth elements in

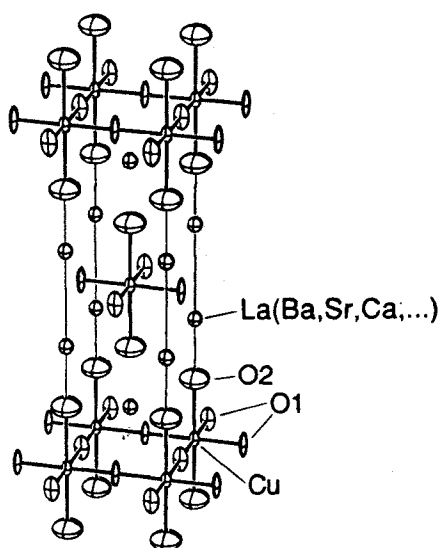


Figure 2. Structure of the "single-layered" $\text{La}_{2-x}\text{R}_x\text{CuO}_4$ compound.

$\text{RBa}_2\text{Cu}_3\text{O}_y$ ($R = \text{Y}, \text{Nd}, \text{etc.}$), a detailed review will be given later.

I.2.3. Bismuth and Thallium copper oxides

The highest values of T_C , currently up to 122 K, are found in a large family of compounds of the type $(\text{AO})_m\text{M}_2\text{-Ca}_{n-1}\text{Cu}_n\text{O}_{2n+2}$ [8,9,10] where the A cation can be Tl, Pb, Bi, or a mixture of these elements, the value of m is 1 or 2 (but is only 2 when A is Bi), the M cation is Ba or Sr, and the substitution of Ca by Sr is frequently reported. The number of CuO_2 layers, separated by Ca, within a unit cell is equal to n , and T_C increases with n up to $n = 3$. For this series, T_C , n , and m values are listed in Table 3[11]. The structures of these compounds are shown in Fig.3[12].

I.2.4. Some other superconducting oxides

A new series of superconductors was discovered with the formula $\text{Pb}_2\text{Sr}_2(\text{Ca},\text{R})\text{Cu}_3\text{O}_{8+x}$ where R can be a variety of rare earths.[13] Its structure is shown in Fig.4 Superconducting onsets in this series occur at temperatures as high as 78 K, but zero resistance has not yet been obtained above 55 K. Although the T_C 's of these materials do not set any records, the compounds give new insight into high-temperature superconductivity. The discovery offers more evidence for what superconductivity researchers already believed, that

Table 3. $(AO)_m M_2 Ca_{n-1} Cu_n O_{2n+2}$ phases [11]

Compound	T_C (K)	n	m
<hr/>			
TlBa ₂ YCu ₂ O ₇	NSC*	2	1
TlBa ₂ CuO ₅	NSC	1	1
TlBa ₂ CaCu ₂ O ₇	90	2	1
TlBa ₂ Ca ₂ Cu ₃ O ₉	110	3	1
TlBa ₂ Ca ₃ Cu ₄ O ₁₁	122	4	1
(Tl,Bi)Sr ₂ CuO ₅	50	1	1
(Tl,Bi)Sr ₂ CaCu ₂ O ₇	90	2	1
(Tl,Pb)Sr ₂ CaCu ₂ O ₇	90	2	1
(Tl,Pb)Sr ₂ Ca ₂ Cu ₃ O ₉	122	3	1
Tl ₂ Ba ₂ CuO ₆	90	1	2
Tl ₂ Ba ₂ CaCu ₂ O ₈	110	2	2
Tl ₂ Ba ₂ Ca ₂ Cu ₃ O ₁₀	122	3	2
Tl ₂ Ba ₂ Ca ₃ Cu ₄ O ₁₀	119	4	2
Bi ₂ Sr ₂ CuO ₆	12	1	2
Bi ₂ Sr ₂ CaCu ₂ O ₈	90	2	2
Bi ₂ Sr ₂ Ca ₂ Cu ₃ O ₁₀	110	3	2
Bi ₂ Sr ₂ Ca ₃ Cu ₄ O ₁₂	90	4	2
Bi ₂ Sr ₂ YCu ₂ O ₈	NSC	2	2

* NSC means non-superconductor.

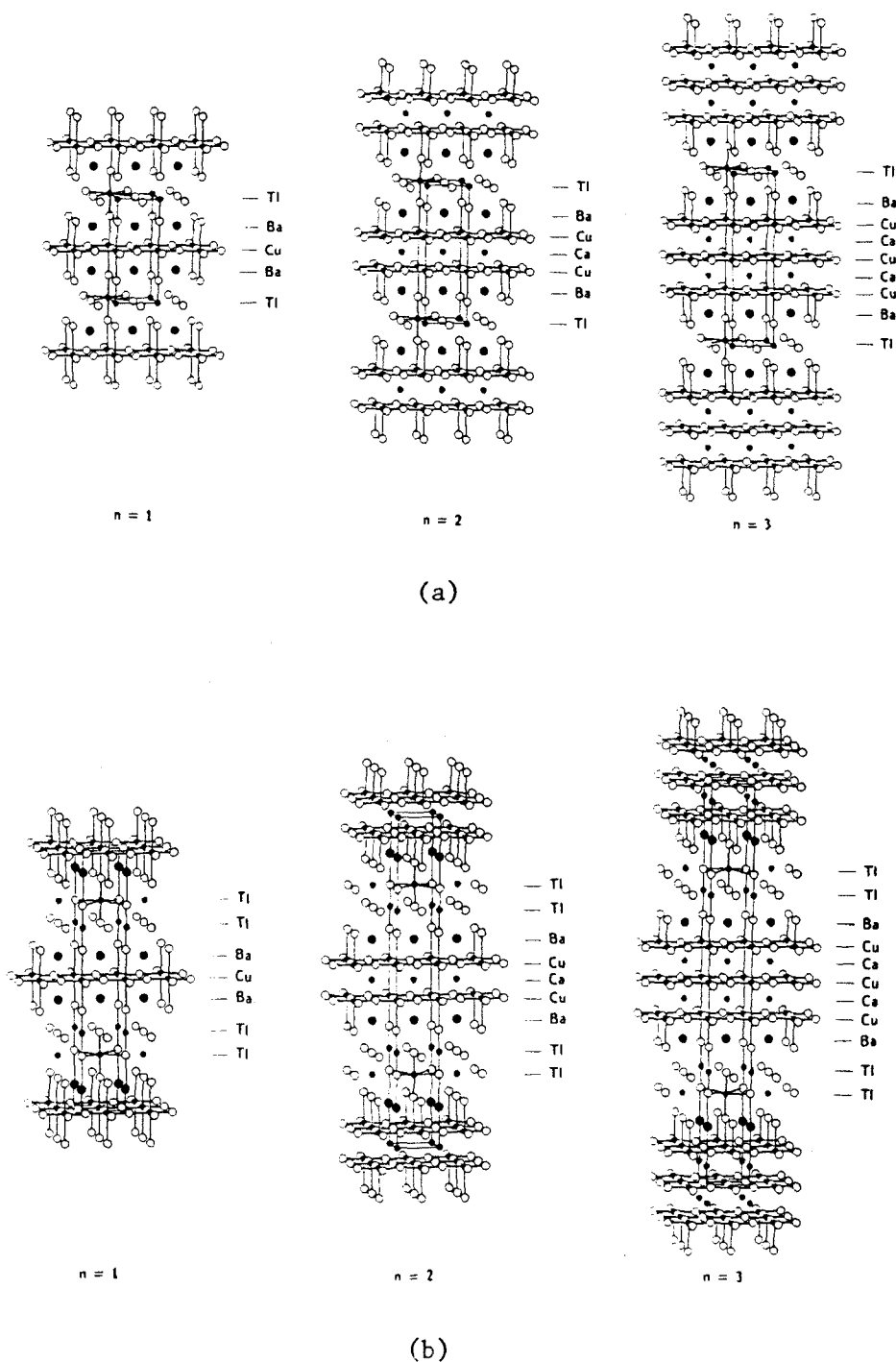


Figure 3. Structure of the "multilayered" $Tl_mCa_{n-1}Ba_2Cu_{n-2n+m+2}$ or $Bi_mCa_{n-1}Sr_2Cu_nO_{2n+m+2}$ compounds: (a) for $m = 1$; (b) for $m = 2$. (from ref.12)

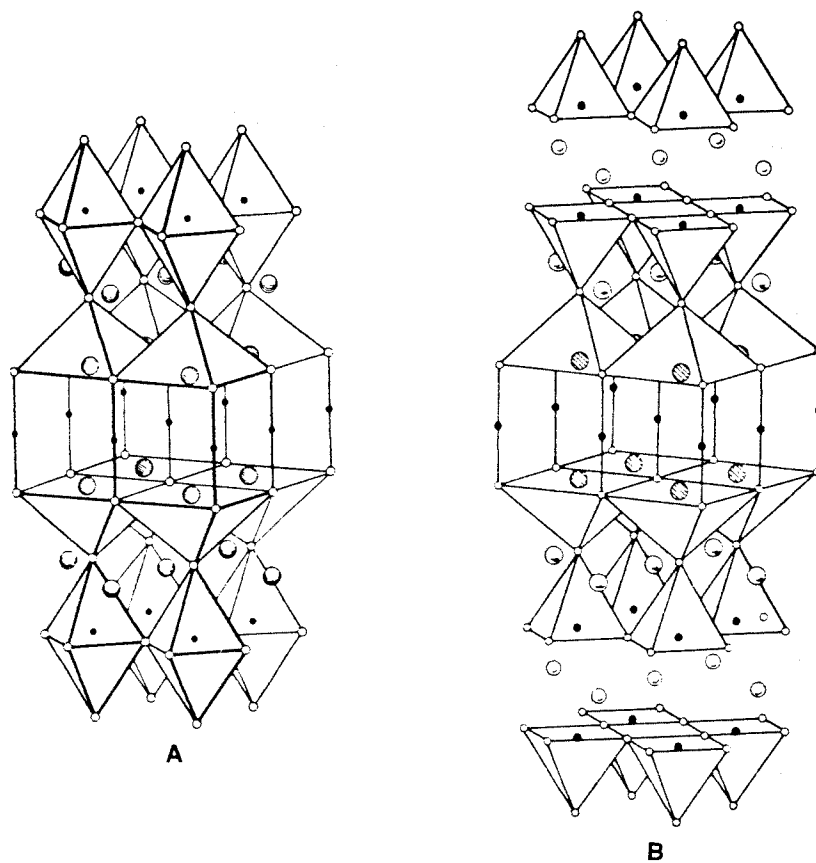


Figure 4. Members of the family $\text{Pb}_2\text{M}_2\text{M}'_{n-1}\text{Cu}_{n+1}\text{O}_{4+2n+x}$ for $n = 1$ (a) and $n = 2$ (b). Small black circles are Cu; small open circles, O; large shaded circles, Pb; large open circles, M and M' (M = Sr and La, M' = Y and Ca). From Cava. [14]

double pyramidal layers of Cu-O such as those found in the new materials play a crucial role in high T_C .

One of the most striking aspects of all presently known high- T_C superconductors with T_C 's greater than 30 K is that they are complex copper oxides with layered perovskite-like crystal structures, all possessing CuO_2 planes. However, like its predecessor $\text{Ba}(\text{Pb}_{1-x}\text{Bi}_x)\text{O}_3$ with a maximum T_C of 13 K, the newly found system $(\text{Ba}_{1-x}\text{K}_x)\text{BiO}_3$, with a maximum T_C near 30 K, has a cubic perovskite crystal structure.[15,16]

It was found that superconductivity in oxide materials very often has an intimate relationship with the perovskite structure. Among the new high- T_C oxides, $\text{YBa}_2\text{Cu}_3\text{O}_y$ has a relatively simple and easily seen structure. Since the research work in this thesis will deal largely with these topics, it is necessary to give a further detailed review of them here.

I.3. Perovskite Structure and Superconductivity

I.3.1. Perovskite structure and $\text{Ba}(\text{Pb},\text{Bi})\text{O}_3$ superconductor

The ideal undistorted perovskite ABO_3 structure (Fig.5) consists of a regular array of equally dimensioned BO_6 octahedra sharing all corner oxygens with neighboring equivalent octahedra, with 180° B-O-B angles. The A-atom site occurs at the center of the large resultant cavity. This ideal ABO_3 array has simple cubic symmetry.

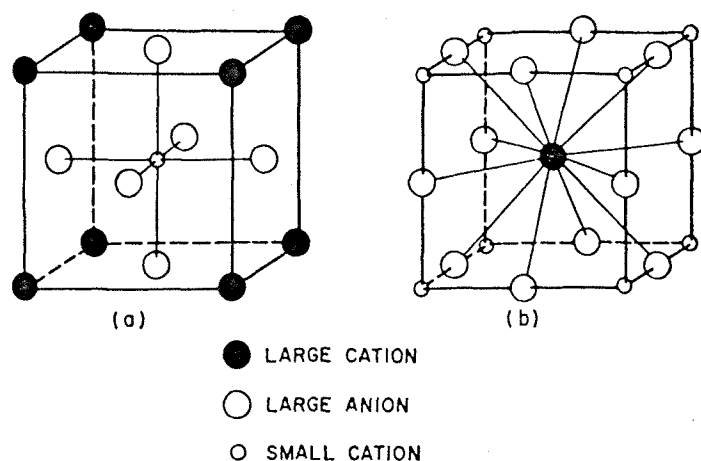


Figure 5. The primitive cubic unit cell of a perovskite compound ABO_3 drawn with two different origins to show coordination about the large(A) and the small(B) cations: (a) the small cation is surrounded by an octahedron of six anions; (b) the large cation is surrounded by twelve anions. [17]

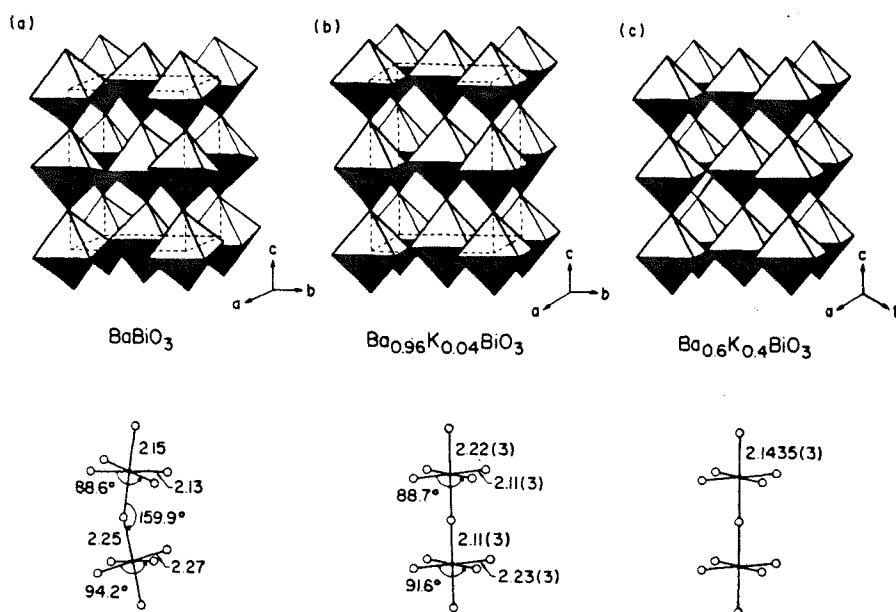


Figure 6. Crystal structures of several members of the $Ba_{1-x}K_xBiO_3$ series: (a) $x = 0$, (b) $x = 0.04$, and (c) $x = 0.40$. Unit cells are indicated by dotted lines in upper figure. Bismuth-oxygen bonding is depicted in the lower figure. From Schneemeyer et al. [16]

Before the pioneering work of Bednorz and Müller, oxide superconductors were well known, but perhaps not fully appreciated.[18,19,20,21] Superconductivity was found in several systems (Table 4), i.e. SrTiO_{3-x} ,^[18] TiO_x ($0.8 < x < 1.30$),^[19] the Li-Ti-O system,^[20] and the Ba-Bi-Pb-O system^[21]. Most anomalous among those superconductors was the perovskite structure material $\text{BaPb}_{0.75}\text{Bi}_{0.25}\text{O}_3$, with a superconducting transition temperature (T_C) of 13 K.^[21]

Table 4. T_C and structure for low- T_C superconducting oxides

Compound	Structure	T_C (K)	Reference
SrTiO_{3-x}	Perovskite	0.3	[18]
TiO_x ($0.8 < x < 1.3$)	Cubic(NaCl)	1.0	[19]
$\text{Li}_{1+x}\text{Ti}_{2-x}\text{O}_4$ ($0 < x < 1/3$)	fcc spinel	7 - 13.7	[20]
$\text{BaPb}_{0.75}\text{Bi}_{0.25}\text{O}_3$	Perovskite	13	[21]

$\text{BaPb}_{1-x}\text{Bi}_x\text{O}_3$ solid solutions derive from the parent compounds BaBiO_3 and BaPbO_3 . Unlike the ideal perovskite structure, in BaBiO_3 larger and smaller BiO_6 octahedra alternate, Bi-O-Bi bond angles deviate from 180° (Figure 6), and the symmetry is reduced to monoclinic.^[22] This very

large structural distortion is considered to be driven electronically, due to the fact that Bi prefers to charge-disproportionate into more highly charged (smaller octahedron) and more weakly charged (larger octahedron) ions rather than sustain a uniform " Bi^{4+} " charge state. Recent careful neutron diffraction studies conclude that the formal charges of the two types of Bi are " $4.5+$ " and " $3.5+$ ". Interestingly, dependent on preparative conditions, the charge disproportionation can occur in either a structurally ordered or structurally disordered manner.[23]

A.W.Sleight et al[22] found that BaPbO_3 is orthorhombic and has a distorted perovskite-type structure in which the Pb atoms occupy one set of equivalent positions with the surrounding O octahedra tilted roughly 8° about a pseudocubic [110] axis. Superconductivity occurs in $\text{BaPb}_{1-x}\text{Bi}_x\text{O}_3$ for compositions near $x = 0.25$. The superconducting region is characterized by a tetragonal structure at 25°C . In $\text{BaPb}_{0.7}\text{Bi}_{0.3}\text{O}_3$ the O octahedra are tilted roughly 8° about the [001] axis. For x between 0.4 and 0.75, orthorhombic symmetry is once again observed. The evolution from the charge-disproportionated pure Bi compound (BaBiO_3) to the metallic pure Pb compound (BaPbO_3) has been the subject of considerable study.[24] If suppression of the charge disproportionation through doping is critical to the superconducting mechanism, then it is remarkable that one must have so much Pb present to achieve that result.

I.3.2. (Ba,K)BiO₃ superconductors

Ba(Pb,Bi)O₃ is made superconducting by the mixing of atoms on the electronically active perovskite B sites. For copper-oxide based superconductors, dopants on the Cu sites are usually detrimental to superconductivity, and A site doping is preferred. Large atom-site doping of BaBiO₃ could involve either partial M³⁺/Ba²⁺ or M¹⁺/Ba²⁺ substitution, introducing holes or electrons.

After many efforts, a series of compounds of A site doping, Ba_{1-x}K_xBiO₃, was finally synthesized.[15,16,25] Bulk superconductivity with a T_c near 30 K occurs for the single-phase simple cubic perovskite Ba_{0.6}K_{0.4}BiO₃, a new compound but obviously intimately related to BaPb_{0.75}Bi_{0.25}O₃.

The crystal structures of various members of the Ba_{1-x}K_xBiO₃ series of compounds are presented in Figure 6. Apparently, a continuous series of perovskite compounds occurs for Ba_{1-x}K_xBiO₃, at least for 0.0 < x < 0.4, with the only differences being in the sizes and shapes of the Bi-O octahedra and the Bi-O-Bi angles, in a manner analogous to what is observed in Ba(Pb,Bi)O₃. What is known about the Ba_{1-x}K_xBiO₃ phase diagram at present can be summarized as follows:

- x=0 : monoclinic, bronze color, semiconducting;
- x=0.04: orthorhombic, black;
- x=0.13: cubic, black, not superconducting;
- x=0.40: cubic, black, superconducting.

Unlike $\text{Ba}(\text{Pb},\text{Bi})\text{O}_3$, very little hole doping is required to suppress the charge-disproportionation almost completely in the $(\text{Ba},\text{K})\text{BiO}_3$ series.

I.4. $\text{YBa}_2\text{Cu}_3\text{O}_y$ Structures, Structure Transitions and Substitutions

As the first superconductor with T_C above the boiling point of nitrogen, $\text{YBa}_2\text{Cu}_3\text{O}_y$ has been the subject of very considerable study.

I.4.1. $\text{YBa}_2\text{Cu}_3\text{O}_y$ structures

$\text{YBa}_2\text{Cu}_3\text{O}_y$ and related "123" oxides have oxygen-deficient perovskite structures.[26,27] A $\text{Cu}^{2+}/\text{Cu}^{3+}$ mixture also exists in these compounds. One structure form is orthorhombic (Figure 7), by virtue of the preferential population of the O1 sites (along the b axis) giving rise to Cu-O chains. A disordered orthorhombic structure can result if both the O1 and O5 sites are occupied (but unequally). A tetragonal structure results if the O1 oxygens are extensively depleted or the O1 and O5 sites are equally occupied. The orthorhombic structure of $\text{YBa}_2\text{Cu}_3\text{O}_y$ continues down to $y = 6.4$ at which point the structure becomes tetragonal; $\text{YBa}_2\text{Cu}_3\text{O}_6$ is tetragonal and nonsuperconducting. The T_C of orthorhombic $\text{YBa}_2\text{Cu}_3\text{O}_y$ shows an interesting variation with y . The T_C is 90 K down to $y = 6.8$; there is a plateau in T_C (55 ± 5 K) in the range of $y = 6.8 - 6.6$. The material becomes nonsuperconducting at $y = 6.4$.

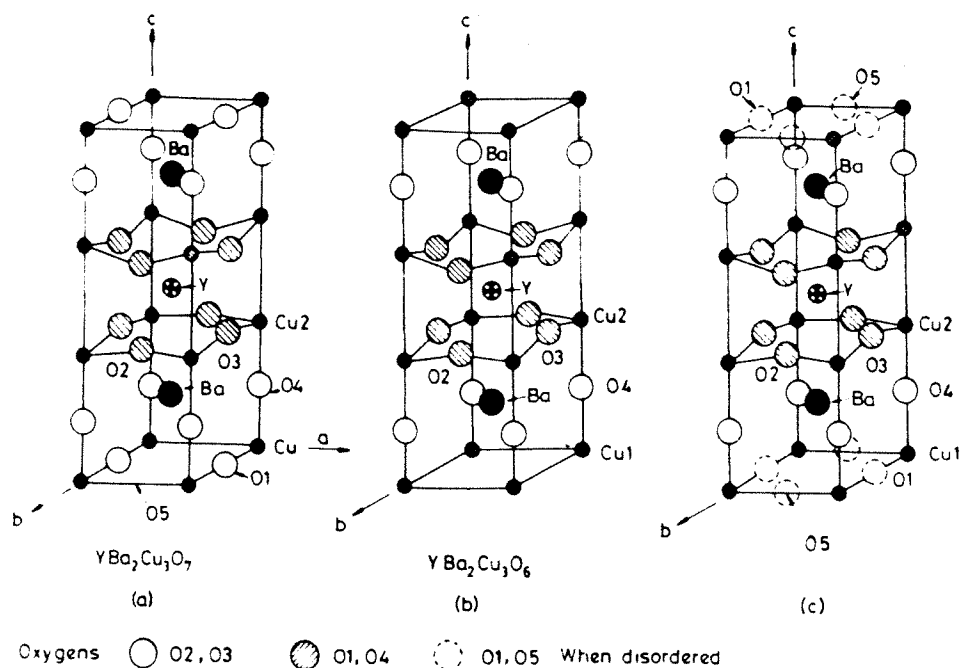


Figure 7. Structure of "double-layered" $\text{YBa}_2\text{Cu}_3\text{O}_y$: (a) $y = 7$, orthorhombic with oxygens ordered on O1 sites; (b) $y = 6$, tetragonal with fully depleted O1 sites; (c) disordered tetragonal structure where both O1 and O5 sites are occupied. From Rao and Raveau. [28]

It was found that the value of y depends on the method of preparation. For example, the oxygen-annealed, slow-cooled materials are usually orthorhombic and superconducting with larger y values; but the oxygen-annealed, fast-cooled materials are orthorhombic with smaller y values or tetragonal so that they present a semiconducting or nonsuperconducting behavior.^[29] It is necessary to have a detailed look at the topic of orthorhombic-tetragonal transition in $\text{RBa}_2\text{Cu}_3\text{O}_y$ compounds to understand the relation between thermal history and superconductivity of the compounds.

I.4.2. Orthorhombic - tetragonal transition in $\text{RBa}_2\text{Cu}_3\text{O}_y$

Like the 40 K compound of $\text{La}_{2-x}\text{Sr}_x\text{CuO}_4$ ($x = 0.15$), the $\text{YBa}_2\text{Cu}_3\text{O}_y$ phase is called an oxygen-defect perovskite because there are only seven oxygens per formula unit instead of the nine required for a triple-cell perovskite. Its crystal structure (Fig.7) consists of a stack of Y, CuO_2 , BaO, CuO, BaO, CuO_2 and Y planes perpendicular to the c -axis, with an ordering of all the oxygen vacancies in the Cu-O median plane resulting in Cu-O chains running along the b -axis.

The wide range of T_c 's reported for single-phase 90 K materials strongly suggested a problem with stoichiometry associated with the processing parameters, particularly the ambient, the annealing temperature, and the cooling rate. The importance of the oxygen ambient and annealing temperature was studied by Tarascon et al^[30] [Fig.8(a)]. It shows the weight loss of an as-grown material heated to 850°C in

argon, cooled in the same ambient to room temperature, and reheated in oxygen to 850°C. The weight lost by the compound (corresponding to one oxygen per formula unit) when heated under argon is equal to the weight gained when heated under oxygen. This indicates a completely reversible loss-insertion process. The TGA (thermogravimetric analysis) trace (at 10°C/min) shows a maximum at 540°C when the sample is heated under O₂, indicating a maximum oxygenation rate at this temperature. This processing temperature region is now widely used to optimize the material's oxygen content and thereby its T_C.

The effect of the synthesis cooling rate is shown in Fig.8(b), where a vacuum-annealed sample is first heated under air, quenched under air, reheated under air, and finally slowly cooled. The difference in oxygen content of 0.3 oxygen atoms per unit formula between the cooled and quenched states clearly illustrates the importance of the cooling rate.

Changes in oxygen content such as these markedly affect T_C, as are shown in Figs. 9 and 10. The vacuum-annealed sample exhibits semiconducting behavior. The metallic behavior and superconductivity can be fully recovered by either thermal annealing in O₂ or the plasma oxidation method^[31]. Therefore, the electrical behavior, concomitant with the oxygen content, of these materials is reversible.

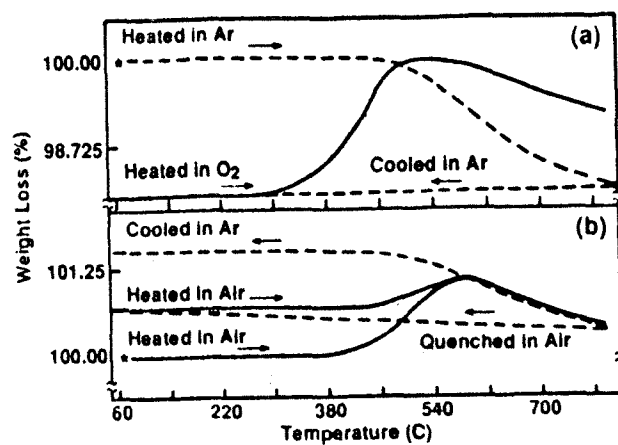


Figure 8. Thermogravimetric analysis (TGA) trace for a $\text{YBa}_2\text{Cu}_3\text{O}_y$ sample (a) annealed in Ar, cooled in Ar and reheated in oxygen, and for a sample (b) annealed in vacuum, heated in air, quenched in air, reheated in air, and finally slowly cooled.[30]

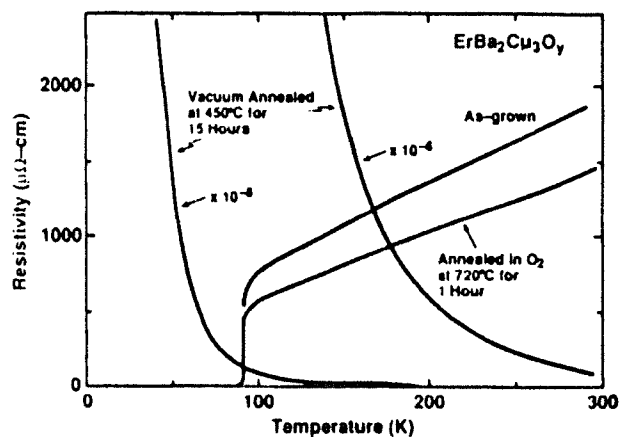


Figure 9. Effect of processing treatments (vacuum annealed and re-annealed in oxygen) on the resistivity temperature dependence of an $\text{ErBa}_2\text{Cu}_3\text{O}_y$ sample. [30]

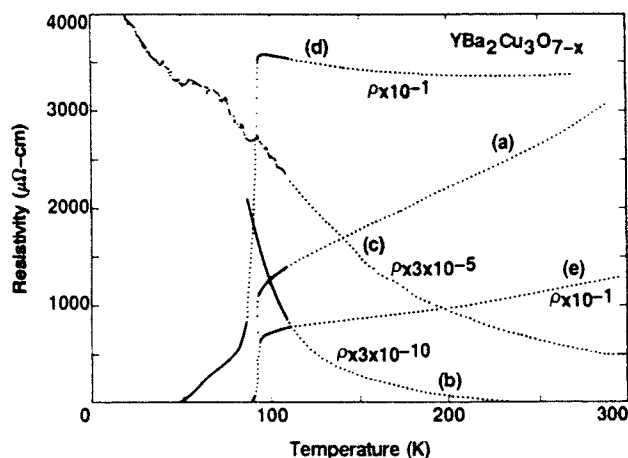


Figure 10. Effect of changing the oxygen content on the properties of $\text{YBa}_2\text{Cu}_3\text{O}_y$. Shown are the resistivities as a function of temperature for the sample (a) as-prepared, (b) after annealing for 15 h at 450°C in a vacuum of 10^{-3} Torr, (c) after 117 h plasma oxidation, (d) after 210 h plasma oxidation, and (e) after plasma oxidation for 285 h. Note the large scale changes in resistivity. [31]

On removal of oxygen, the basic unit cell evolves from an orthorhombic (O) symmetry at $y = 7$ to a tetragonal (T) symmetry at $y = 6$. Neutron scattering experiments^[32] have shown that the oxygen is removed from the Cu-O chains in the orthorhombic phase and continues until the tetragonal phase is formed, whereupon the oxygen sites in the median CuO plane are equally occupied (i.e., there are no chains) or until, at $y = 6$, there is little or no oxygen left in this plane. This oxygen removal is a function of temperature [as shown in Fig.8(a)] and it has been demonstrated by x-ray diffraction that the O-T transition occurs at $T = 740^{\circ}\text{C}$ and 1 atm O_2 . The synthesis of the bulk $\text{RBa}_2\text{Cu}_3\text{O}_y$ phase by a solid-state reaction generally requires temperatures higher than 900°C and, according to updated information^[30], cannot be lower than 800°C . Thus the initial phase which is formed in the solid-state reaction has tetragonal symmetry which converts to the desired orthorhombic phase on cooling below the O-T transition temperature. On lowering the partial pressure of oxygen from 1 atm to 100 mT, the temperature at which the O-T transition occurs decreases from 740°C to 600°C . Superconducting thin film, in contrast to the preparation of bulk materials, can now be grown at 650°C and 100 mT partial pressure of oxygen.^[30]

Studies^[33,34] of the complete $\text{YBa}_2\text{Cu}_3\text{O}_y$ series have documented in more detail that the oxygen concentration is important, but how and at what temperature the oxygen is removed are also important. It has been shown^[35] that the

composition at which the O-T transition takes place strongly depends on the annealing temperature and that the largest y value at which the O-T transition is obtained is at the highest annealing temperature. Thus the y value alone for an oxygen-depleted $\text{YBa}_2\text{Cu}_3\text{O}_y$ sample is meaningless without the experimental details describing the processing history of the sample and it is only on this basis that different samples can be compared.

Evidence for the existence of two bulk superconducting transitions at 55 K and 90 K in the $\text{YBa}_2\text{Cu}_3\text{O}_7$ system was first observed by Tarascon et al.^[36] in a sample which was vacuum-annealed and subsequently oxidized at low temperatures (Fig.11). The ac-susceptibility trace for this sample shows distinct 55 K and 90 K superconducting transitions with no other transitions apparent. Plasma oxidation at low temperature ($< 80^\circ\text{C}$) also clearly produced superconducting transitions at 55 K and 90 K in the temperature dependence of both the resistivity and ac susceptibility, with no other transitions detected.^[37] From x-ray powder diffraction analysis, the 90 K and 60 K materials appear similar. However, high resolution electron microscopy (HREM) can distinguish between the two phases. At $y = 7$ the oxygen vacancies are ordered in a manner leading to the Cu-O chains parallel to the b -axis. For the $y = 6.5$ sample there is a modulation in the " a " direction corresponding to the occupancy of one out of every two chains, but there is no correlation in the " c " direction.^[38]

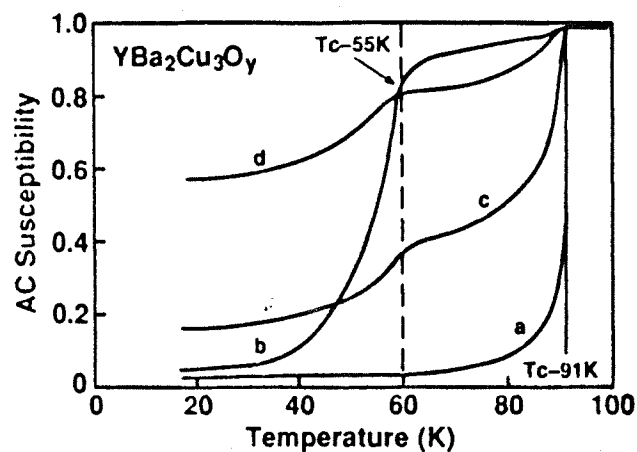


Figure 11. Effect of processing heat treatments on the superconducting properties (ac-susceptibility) of YBa₂Cu₃O_y. Curve (a) is for the as-grown material; Curve (b) is for a vacuum-annealed sample heated in 2×10^{-3} torr oxygen to 800°C at 5°C/min, and cooled at 5°C/min to room temperature. Curve (c) and (d) are vacuum-annealed samples heat treated at 300°C in 10^{-2} torr oxygen for 15 hours (c), and 5 hours (d). [36]

I.4.3. Substitutions in $\text{YBa}_2\text{Cu}_3\text{O}_y$

Since the discovery of high-temperature superconductivity in $\text{YBa}_2\text{Cu}_3\text{O}_7$, many attempts to substitute other elements for Y, Ba or Cu have been made in order to improve its properties, understand the mechanisms of superconductivity of the new oxide materials, and find other new superconducting materials.

I.4.3.1 Copper substitution effects: $\text{YBa}_2(\text{Cu}_{1-x}\text{M}_x)_3\text{O}_y$

Numerous investigations into the effects of the substitution of copper in $\text{YBa}_2\text{Cu}_3\text{O}_y$ by a great variety of metallic elements M have appeared in the literature. By far, the most extensive research performed to date, and that for which the substitutions have resulted in single-phase materials, has been for the substituent elements $M = \text{Fe}, \text{Co}, \text{Ni}, \text{Zn}, \text{Ga},$ and Al .^[39] The rich variety of reported behavior, as well as much of the experimental disagreement, arise primarily from the preferential occupancy of the two inequivalent copper sites. Consideration of the relative substitutional occupancies of the $\text{Cu}_1(\text{chain})$ and $\text{Cu}_2(\text{plane})$ sites (Figure 7) is central to the interpretation of primary features such as the degree of degradation of superconducting properties, the apparent orthorhombic-tetragonal phase transformation, oxygen site occupancy, substitutional solubility, and annealing effects. The dependence of T_c on copper-site dopant concentration is shown in Figure 12 for a variety of substituent species.

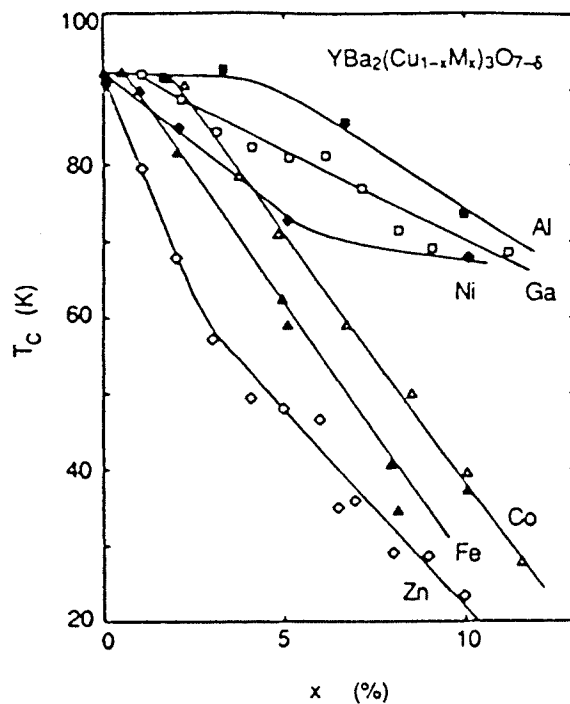


Figure 12. Superconducting transition temperature T_C vs. dopant concentration x for $\text{YBa}_2(\text{Cu}_{1-x}\text{M}_x)_3\text{O}_{7-\delta}$. Data for $M = \text{Al}$ (solid squares), Ga (open squares), Ni (solid diamonds), Co (open triangles), Fe (solid triangles), and Zn (open diamonds) are shown. From Markert et al.[39]

X-ray diffraction data generally indicate that for all trivalent substitutions such as Fe, Co, Al and Ga, an orthorhombic-tetragonal structural phase transition seems to occur near $x = 0.02-0.04$. A significant feature is that superconductivity persists for concentrations far beyond that at which the transition occurs; T_c depression is typically only about 2-5 K/at.%. Neutron diffraction data provide strong evidence that Fe and Co substitute preferentially on the Cu1(chain) site, where they may more readily achieve their preferred octahedral coordination, or slightly displaced from this position, where a distorted tetrahedral coordination can be attained.

In contrast to the trivalent dopants, substitution of divalent Zn for Cu results in an unusually rapid depression of T_c , with a typical value of 11 K/at.%. A single-phase material can be maintained up to about $x = 0.10-0.16$ in $\text{YBa}_2(\text{Cu}_{1-x}\text{Zn}_x)_3\text{O}_y$. The structure, however, remains orthorhombic up to the highest dopant concentrations. Earlier and later neutron diffraction measurements gave different results: one indicates that Zn populates both sites and somewhat prefers Cu1 sites; the other shows Zn occupancy only on the Cu2 site. In either case, it is remarkable that the small concentration of Zn ions on Cu2 sites is responsible for the severe degradation of superconductivity. This unique behavior is often attributed to its filled d-level electronic structure; band-filling of 3d holes decreases the density of states at the Fermi energy. The Zn ions may also

cause local distortions in the Cu₂ planes; such defects are capable of inducing magnetic moments through localization effects, which could conceivably cause magnetic pair-breaking.

Unlike the Zn-substituted species, neutron diffraction measurements indicate that Ni substitutes only at the Cu₂ site. However, for this magnetic ion, superconducting properties degrade less quickly than in the case of nonmagnetic Zn (Fig.12).

The 3d metal substitution studies have helped clarify the relative role of the chains and planes with respect to the superconducting properties. Because a Ni or Zn substitution for Cu in the planes causes T_C to decrease faster with dopant concentration than when the substitution is Co, Fe, or Al for Cu in the chains it was suggested that superconductivity is confined to the CuO₂ planes and the role of the chains is to act as a hole carrier reservoir coupling the planes. Thus a chemical-structural unit (not necessarily a Cu-O chain, e.g. also the BiO or TlO layers in high- T_C bismuth or thallium copper oxides shown in Fig.3), capable of acting as a hole reservoir to provide an electronic coupling between CuO₂ planes, appears to be necessary for the occurrence of superconductivity in these materials.

Partial substitution of the monovalent ion, Li⁺ for Cu in superconducting YBa₂Cu₃O_y has been studied by Suchow et al^[40]. They found that Li ($x < 0.15$) elevates T_C slightly before depressing it (from $x = 0.15$) in nominal YBa₂Cu_{3-x}Li_xO_y.

I.4.3.2. Barium substitution effects

When Ba in $\text{YBa}_2\text{Cu}_3\text{O}_7$ is progressively replaced by an isovalent element, Sr, the T_C is lowered and the resistivity of the material above the critical temperature continuously increases.^[41] In $\text{YBa}_{2-x}\text{La}_x\text{Cu}_3\text{O}_y$, the structure becomes tetragonal with increase in x and the T_C of the orthorhombic phase decreases with increase in x .^[42,43,44,45,46]

I.4.3.3. Substitutions for Y in $\text{YBa}_2\text{Cu}_3\text{O}_y$

Substitution of trivalent Y by ions M of lesser charge in $(\text{Y}_{1-x}\text{M}_x)\text{Ba}_2\text{Cu}_3\text{O}_y$ has been performed for $\text{M} = \text{Ca}$ ^[42,43,47] and $\text{M} = \text{Na}$.^[48] The limit of solubility of Ca for Y has been variously reported as being between $x = 0.2$ and $x = 0.5$; the structure remains orthorhombic over the Ca dopant range, although the orthorhombic distortion slightly decreases. Superconducting transition temperatures remain high. Substitution of Na for Y permits higher solubility, up to $x = 0.5$. For this $(\text{Y}_{1-x}\text{Na}_x)\text{Ba}_2\text{Cu}_3\text{O}_y$ system, little degradation of T_C occurs up to $x = 0.3$, where $T_C = 80 \text{ K}$; however, T_C drops quickly thereafter to about 40 K at $x = 0.5$. The increasing development of magnetic moment with increasing x was observed, which, if not due to impurity phases, may indicate a conversion of Cu^{3+} to Cu^{2+} . Such behavior probably reflects a tendency toward greater oxygen deficiency with increasing dopant concentration.

Isovalent substitutions for Y in $\text{YBa}_2\text{Cu}_3\text{O}_y$ brought about both successful and unsuccessful results in terms of superconductivity. Shortly after $\text{YBa}_2\text{Cu}_3\text{O}_y$ was found, the lanthanide analogues $\text{LnBa}_2\text{Cu}_3\text{O}_y$ with $T_C = 90\text{--}94$ K were discovered, where Ln is a lanthanide element except for Ce, Pr, Pm, and Tb (Pr-123 is nonsuperconducting and Tb-123 and Ce-123 cannot be formed due to the stable tetravalent state of Tb and Ce).^[7]

Substitution of lanthanum for yttrium in $\text{YBa}_2\text{Cu}_3\text{O}_y$ has proven to be unusual among the rare-earth-substituted high- T_C compounds, since $\text{LaBa}_2\text{Cu}_3\text{O}_y$ is a superconductor but with a lower transition temperature, typically around 50 K. The lower T_C correlates with structural properties and has been attributed to disorder on the La and Ba sites [as in the formula $\text{La}(\text{Ba}_{2-x}\text{La}_x)\text{Cu}_3\text{O}_y$] and/or oxygen vacancy disorder. [49,50,51,52,53,54] Because the La^{3+} ion is the largest trivalent ion in the rare-earth series, it most readily substitutes for the larger Ba^{2+} ion so that the stoichiometric $\text{LaBa}_2\text{Cu}_3\text{O}_y$ was not synthesized for a long time. Under special synthesis conditions, a superconducting onset temperature of 95 K and zero resistance temperature of at least 80 K have recently been attained in $\text{LaBa}_2\text{Cu}_3\text{O}_y$.^[55,56,57] Since conventional sintering under an oxygen atmosphere is known to produce $\text{La}_{1+x}\text{Ba}_{2-x}\text{Cu}_3\text{O}_y$, in which La is substituted for Ba in the crystal lattice, a special method called "gas exchange techniques" (Fig.13)^[57] was used to obtain

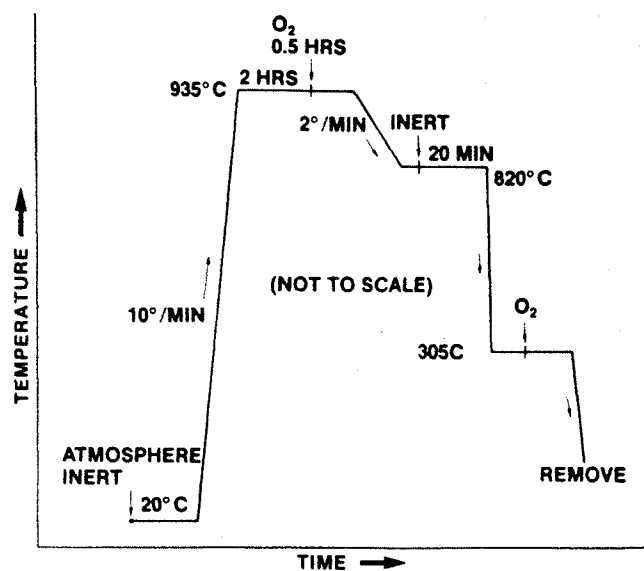


Figure 13. Schematic diagram for high temperature processing of $\text{LaBa}_2\text{Cu}_3\text{O}_y$ with T ($R = 0$) above 90 K. [57]

the stoichiometric $\text{LaBa}_2\text{Cu}_3\text{O}_y$ compound. It was shown that during the initial inert atmosphere sintering step, $\text{LaBa}_2\text{Cu}_3\text{O}_y$ powder decomposes, in part, into several intermediate compounds. These compounds are then recombined in the subsequent oxygen atmosphere sintering step to form $\text{LaBa}_2\text{Cu}_3\text{O}_y$, which achieves zero resistance at temperature above 90 K. It was proposed that the net effect of these two processing steps is to inhibit the substitution of La for Ba in the fully processed material.

I.5. Substitution of Bi for Y: Questions and Significance

The substitution of Bi for Y (or other rare earth elements, e.g. Nd) in $\text{RBa}_2\text{Cu}_3\text{O}_7$ ($R = \text{Y, Nd, etc.}$) is particularly interesting because there are significant aspects in practical applications and theoretical studies.

I.5.1. Substitution of Bi for Y: a possibility

The most serious problem in practical applications of $\text{YBa}_2\text{Cu}_3\text{O}_7$ relates to the low critical current densities (generally of the order 10^7 A m^{-2}) observed in polycrystalline ceramic samples.[58,59] These values compare with 10^9 - 10^{11} A m^{-2} reported for single-crystal, thin-film samples.[60,61] The major cause of this problem is probably the presence of non-superconducting or insulating barriers between the superconducting grains in sintered specimens. Whereas the replacement of yttrium with other rare-earth elements has shown no improvement in critical current

densities or room temperature resistivities, it was reported that Bi substitution resulted in an improvement of inter-grain contact in this polycrystalline material and reduced the normal state resistivity by factors of 2 to 7. [62,63,64] This effect was rationalized in terms of the low melting point of the Bi_2O_3 starting material causing it to act as a flux during the sintering process. In this way, it seems to be possible to bring about a large increase in the low critical current densities of this new ceramic superconductor and make its use practical.

Due to the important implications of these observations, many researchers conducted re-examinations of the structural and electrical effects of Bi substitution in $\text{YBa}_2\text{Cu}_3\text{O}_y$. [65,66,67] The results concluded that no significant degree of doping could be obtained before phase segregation occurred. The minority phase has been identified as Ba_2BiYO_6 , and its structure(cubic) has been shown by powder X-ray diffraction to be based on perovskite, with an ordered arrangement of Bi^{5+} and Y^{3+} in the octahedral sites. This phase is insulating, and its presence in $\text{YBa}_2\text{Cu}_3\text{O}_y$ samples results in an increase in the normal-state resistivity.

As an unidentified phase, Ba_2BiYO_6 was first found by Spencer and Roe^[68], who determined $a = 8.55$ Å. Blower et al [65] first gave a detailed procedure of Ba_2BiYO_6 structure refining and its structure (Fig.14): face centered cubic, $\text{Fm}\bar{3}\text{m}$, $a = 8.5675(6)$ Å. Zhuang et al [66] obtained the same space group, $\text{Fm}\bar{3}\text{m}$ and a lattice constant with little diffe-

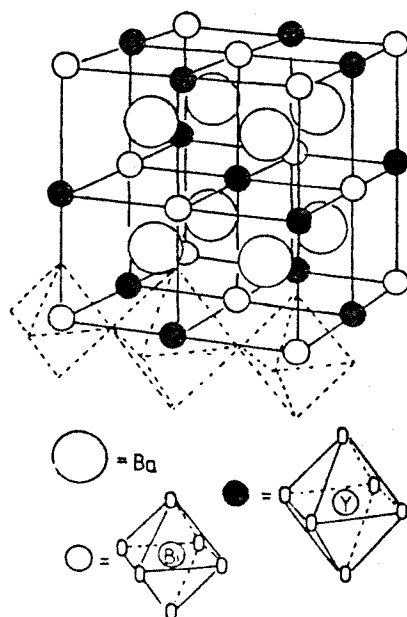


Figure 14. Structure of Ba_2BiYO_6 . From Blower and Greaves. [65]

rence, $a = 8.549$ Å. The fact that Ba_2BiYO_6 is not superconducting perhaps provides more evidence for the assumption that superconductivity occurs within the framework of a three dimensionally connected bismuth-oxygen array in the simple perovskite bismuth oxide-based superconductors mentioned above.

In spite of the conclusions, there are still some questions unanswered. It is noted that all Bi substitution experiments conducted by former researchers were carried out under oxidizing conditions (in air or O_2). In starting material Bi_2O_3 , Bi is $3+$; but in Ba_2BiYO_6 , Bi is $5+$. If Bi^{3+} can be prevented from being oxidized to Bi^{5+} , it may be possible to prevent the non-superconducting phase, Ba_2BiYO_6 , from forming and to insert Bi^{3+} into the Y sites.

In the $\text{YBa}_2\text{Cu}_3\text{O}_y$ structure, the rare earth ion is 8-fold coordinated (Fig.7). The differences between the effective ionic radii (Table 5)^[69] of Bi^{3+} and Y^{3+} , or Nd^{3+} , or La^{3+} in C.N.= 8 are $[(1.17-1.019)/1.0945]100\% = 13.8\%$, or $[(1.17-1.109)/1.1395]100\% = 5.4\%$, or $[(1.17-1.16)/1.165]100\% = 0.9\%$, respectively, which are less or much less than the "maximum 15% rule" for solid solution formation. The difference between the ionic radii of Tl^{3+} and Y^{3+} (C.N.=8) is $[(1.019-0.98)/0.9995]100\%=3.9\%$, also smaller than the maximum-permitted 15%. From the views of charge and radius, the substitution of Bi for trivalent rare earth, Y, or Nd, or La in the $\text{RBA}_2\text{Cu}_3\text{O}_y$ structure seems to be possible if Bi^{3+} can be prevented from forming Bi^{5+} . The substitution of Tl

Table 5. Effective ionic radii ("IR") of selected ions^[69]

Ion	Coordination number (CN)	r (Å)
<hr/>		
Bi ³⁺	6	1.03
Bi ³⁺	8	1.17
Bi ⁵⁺	6	0.76
<hr/>		
Cu ²⁺	4	0.57
Cu ²⁺	4 (square)	0.57
Cu ²⁺	5	0.65
Cu ²⁺	6	0.73
Cu ³⁺ (low-spin)	6	0.54
<hr/>		
La ³⁺	6	1.032
La ³⁺	8	1.160
<hr/>		
Nd ³⁺	6	0.983
Nd ³⁺	8	1.109
<hr/>		
Tl ³⁺	6	0.885
Tl ³⁺	8	0.98
<hr/>		
Y ³⁺	6	0.900
Y ³⁺	8	1.019

for Y is probably much easier to realize since Tl^{3+} cannot be oxidized to Tl^{5+} but it can, unlike Bi, go to the +1 state.

$NdBa_2Cu_3O_Y$ is isostructural with and exhibits properties similar to those of $YBa_2Cu_3O_Y$.^[8,70] It was found that, under certain conditions, the Nd-Ba-Cu-O system is more favorable than the Y-Ba-Cu-O system for the formation of the 123 superconductor.^[71] This is another reason besides the factor of atomic sizes why the Nd-123 material was the primary focus in our research of the possible substitution of Bi for the rare earth ions in the $RBa_2Cu_3O_Y$, which is a main topic of this thesis.

It should be pointed out that, although there is an advantage for Bi^{3+} to replace La^{3+} in $LaBa_2Cu_3O_Y$ from the radius viewpoint, substitution of Bi^{3+} for La^{3+} in $LaBa_2Cu_3O_Y$ is not a main topic of this thesis because, as mentioned above, pure $LaBa_2Cu_3O_Y$ cannot be easily obtained.

I.5.2. Substitution of Bi for Y: significance

Bi and Tl possess some chemical and physical properties, for example, electron structures, ionic sizes and electronegativity, etc. which are different from Y and other rare earth elements. As mentioned above, Bi and Tl raise T_C in the other layer-structure compounds (Bi- and Tl-copper oxides). If Y or some other rare earth elements in the 123 superconductors can really be replaced by Bi or Tl, some changes in the properties, e.g., T_C of the superconducting

materials, might result so that the relationship between the chemical and physical properties of the elements and the superconductivity will be revealed.

Recently, some very interesting relations between superconductivity and electronegativity of materials including elemental, non-oxide, and oxide superconductors have been found.[72,73,74,75,76]

A striking feature observed was that the average electronegativity (χ) of the different oxide superconductors lies in a very narrow range from 2.50 to 2.65 while the conventional non-oxide superconductors have χ -values well below that of the oxide systems and, on the other hand, the nonsuperconducting oxides with perovskite structure are found to have χ -values above those of the oxide superconductors.[73] It was proposed that one of the criteria for oxide materials to be superconductors is that their average values should be in the range 2.5-2.65.

Nepela and McKay [76] also studied the correlation of electronegativity and T_C of the new oxide superconductors. They chose the difference ($\Delta\chi$) between the average electronegativity of all anions and the average electronegativity of all cations in the compounds instead of the average electronegativity of all ions (positive and negative) to demonstrate the relation between electronegativity and T_C . They found that, for copper-based and some other compounds, T_C scales linearly with $\Delta\chi$, i.e. T_C increases as $\Delta\chi$ becomes larger (Fig.15).

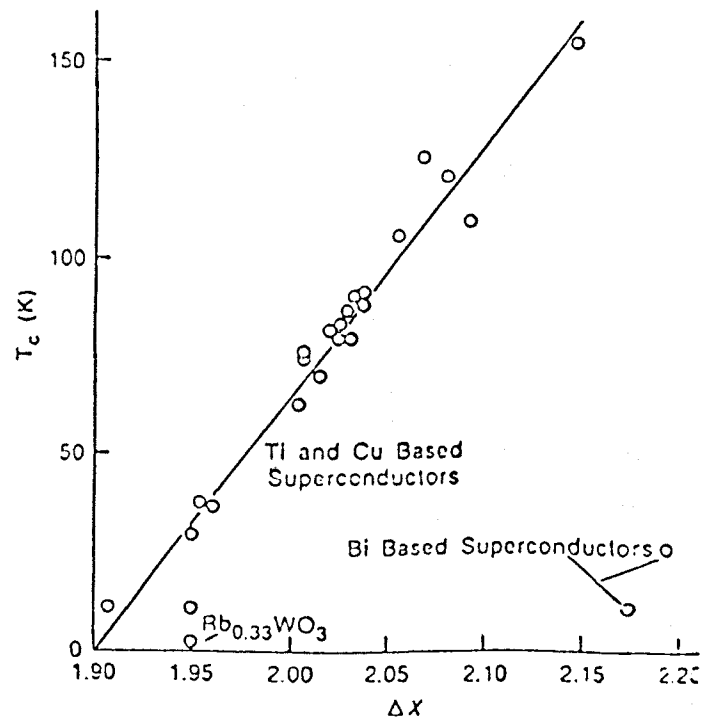
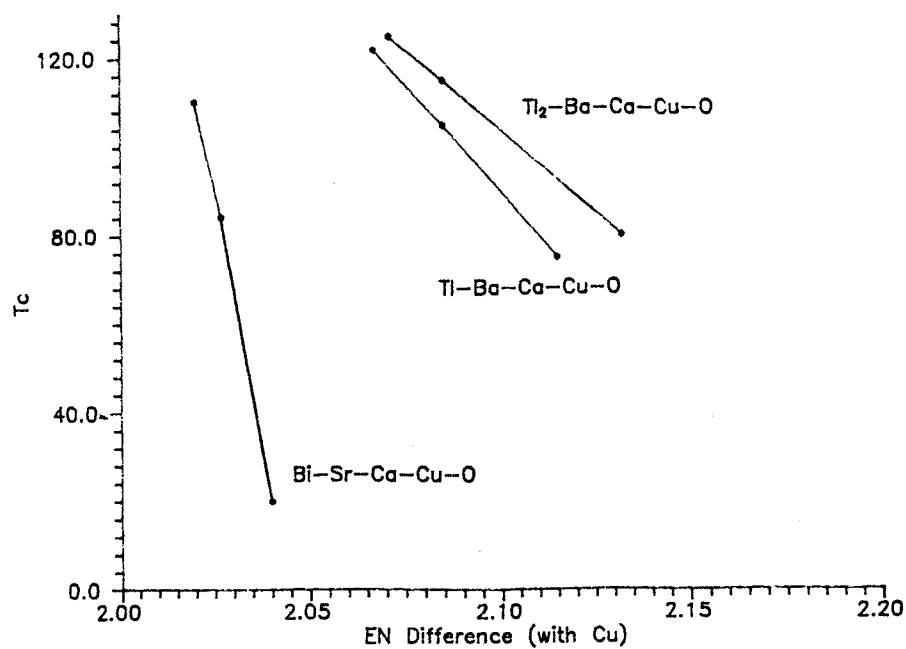


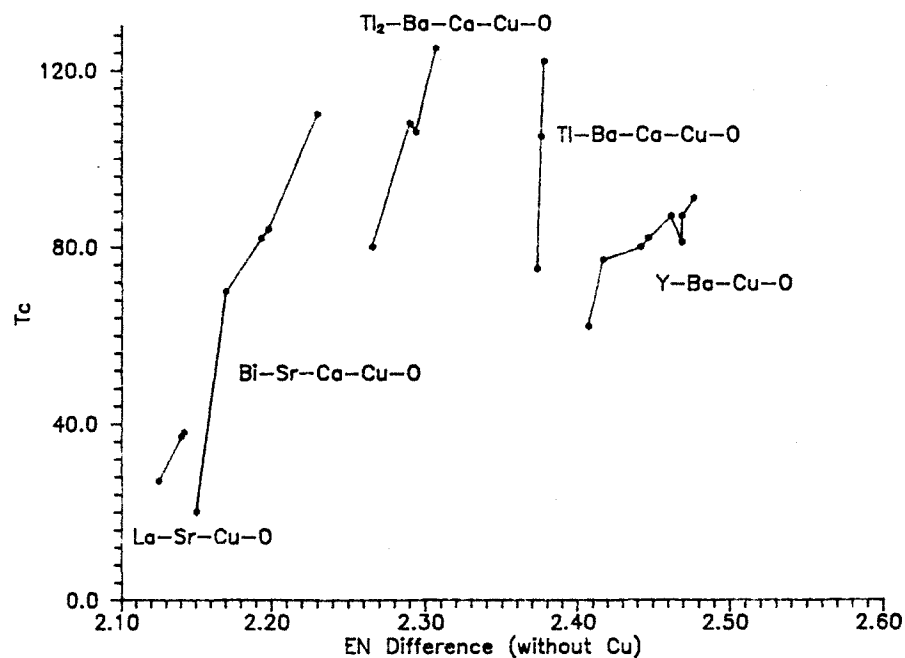
Figure 15. T_c as a function of $\Delta\chi$ for some high-temperature superconductors. From Nepela and McKay.[76]

By recalculating the $\Delta\chi$ of some superconducting Cu-O systems, however, we found that the above conclusion does not hold (Fig.16) unless Cu is omitted from the calculation of $\Delta\chi$. It can be seen that, for all Cu-O superconducting systems shown in Fig.16, T_C increases as $\Delta\chi$ (without Cu) increases in the same series. This means that, in the same system, the more ionic the compound, the higher its T_C . Indeed, this result agrees with the calculation employing average electronegativity mentioned above.

Although so much information has been gathered, in order to obtain direct evidence of effects of electronegativity on T_C , it appeared desirable that further studies be made. For example, if Bi or Tl, with higher electronegativity (Table 6)[77] can be substituted for Y, Nd, or other rare earth ions, the effects could be examined directly. Gordy [78] proposed that the physical meaning of the electronegativity is the effective electric potential acting on bonding electrons at a crystal lattice point. Our study could, therefore, contribute to understanding the connection between the electrostatic action of electrons to crystal lattice and superconductivity. It was also hoped that the study would provide guidance for formulation of compounds with higher T_C .



(a)



(b)

Figure 16. T_c as a function of electronegativity (EN) difference for some oxide high- T_c superconductors. (a) T_c vs. EN difference calculated with Cu; (b) T_c vs. EN difference calculated without Cu.

Table 6. Electronegativity of selected elements^[77]

Element	Electronegativity
Y	1.2
Nd	1.1-1.2
La	1.1-1.2
Bi	1.9
Tl	1.8
Ba	0.9
Cu	1.9
O	3.5

II. EXPERIMENTAL

II.1. Sample Preparations

Preparations, based on the general formula $R_{1-x}Bi_xBa_2Cu_3O_y$ ($R = Y, Nd$, etc.) with x -values from 0 to 1, were made via several steps. First, appropriate quantities of Y_2O_3 (99.99%, Research Chemicals) or Nd_2O_3 (99.9%, Research Chemicals), Bi_2O_3 (99.9%, J.T.Baker Chemical Co.), $BaCO_3$ (Mallinckrodt Analytical Reagent) and CuO (Mallinckrodt Analytical Reagent) were ground together thoroughly.

Because Nd_2O_3 usually changes to $Nd(OH)_3$ in air at room temperature, the Nd_2O_3 powder was first placed in an open platinum crucible and heated at $1200^{\circ}C$ for one hour. X-ray diffraction proved that pure Nd_2O_3 was thus obtained.

The ground mixtures were transferred into open porcelain or high-density alumina crucibles. It was found that a liquid phase usually occurred in the samples containing Bi after reaction above $900^{\circ}C$; in these cases, the alumina crucible was found to be more resistant to chemical attack than the porcelain crucible. It was therefore chosen here in order to prevent contamination of the products.

Synthesis reactions were carried out in a Harper muffle furnace with automatic temperature control ($\pm 10^{\circ}C$) at desired reaction temperatures which depended on sample compositions. For $Y_{1-x}Bi_xBa_2Cu_3O_y$ ($0 < x < 0.5$), the temperature gradient was set at 920° to $970^{\circ}C$, and for $Nd_{1-x}Bi_xBa_2-$

Cu_3O_y ($0 < x < 0.5$), $880\text{--}950^\circ\text{C}$ since the melting point of Nd_2O_3 is lower than that of Y_2O_3 (Table 7) and $\text{NdBa}_2\text{Cu}_3\text{O}_y$ was found to be formed more easily than $\text{YBa}_2\text{Cu}_3\text{O}_y$ at lower reaction temperatures. For the samples in the same system, it was found that, at a given reaction temperature, as more Bi_2O_3 was added, more liquid phase occurred; this resulted in coarse and non-uniform crystal grains and thus poor T_c 's. In order to eliminate this effect and attain uniform crystal grains in samples with different Bi content, desired reaction temperatures were achieved simultaneously by placing different samples at different points along the natural temperature gradient of the furnace; i.e., the pure $\text{YBa}_2\text{Cu}_3\text{O}_y$ (or $\text{NdBa}_2\text{Cu}_3\text{O}_y$) at the highest temperature position and the sample with maximum Bi ($x = 0.5$, for example) at the lowest temperature region. The samples were kept at these temperatures for 10 - 20 hours to effect complete reaction and then rapidly cooled by removing them from the hot furnace (i.e. air-quenching), or else slowly cooled by leaving them in the furnace with the power off overnight. Any special reaction atmosphere other than air was obtained by passing the special gas over the reactant mixtures in a one-end-closed combustion tube in the muffle furnace. The cooled samples were reground and shaped into 1/2-inch-diameter discs in a cylindrical die in a Carver hydraulic press at a pressure of 0.14 - 0.28 GPa ($2.0 - 4.0 \times 10^4$ lbs/in²). The pellets were then placed in the furnace or the

Table 7. Melting points of selected compounds^[79]

Compound	Melting Point(°C)	Compound	Melting Point(°C)

Bi ₂ O ₃	825±3	BaCO ₃	1740
CuO	1326	Gd ₂ O ₃	2330±20
La ₂ O ₃	2307	Nd ₂ O ₃	2272±20
Tl ₂ O ₃	717±5	Y ₂ O ₃	2410

combustion tube at the same temperature and in the same atmosphere as in the prereactions for 1 - 4 hours for final sintering and then they were cooled slowly in the furnace to below 400°C to ensure the formation of the orthorhombic structure for the samples reacted in air. In order to increase oxygen content or reintroduce oxygen, some samples were annealed in air or O₂ (flow rate 31 cc/min.) at 250 - 500°C for several hours up to several weeks.

II.2. X-ray Diffraction Investigations

All of the prepared samples were studied by the x-ray diffraction powder method to obtain information on phase compositions and structures of the samples. CuK α radiation and 57.3 mm-diameter Philips powder cameras were employed. Experimental parameters were as follows:

accelerating voltage: 35 kvolts; lamp current: 15 mA;

filter: Ni; film exposure time: usually 5 hours.

The x-ray patterns obtained were first measured and then compared with the data of related compounds documented in the literature (see APPENDIX I) or, simply, compared with the x-ray patterns of some pure compounds, which were measured by the same x-ray machine as the samples, to identify the crystal phases formed.

II.3. Microscopy

An optical transmission microscope was used to identify different phases with different colors in the samples. The magnification used was 440x. In order to obtain a clear image, the oil immersion method was adopted.

II.4. Thermogravimetric Analysis (TGA)

A TGA7 Thermogravimetric Analyzer (Perkin-Elmer) was used to study the processes of oxygen absorption by oxygen-deficient phases on annealing. Heating rate was 40°C/min. Heating was performed from room temperature to 800°C in an atmosphere of air. Sensitivity of the thermal balance used is 0.001 mg.

Samples were heated in an oven at 150°C for more than 2 hours to eliminate any moisture in the samples before thermogravimetric analysis. The weight of each sample tested was approximately 80 mg. From $\text{RBa}_2\text{Cu}_3\text{O}_6$ to $\text{RBa}_2\text{Cu}_3\text{O}_7$, the weight change is 16 atomic units. Therefore the absolute weight change for 80 mg of $\text{YBa}_2\text{Cu}_3\text{O}_6$ (formula weight=650.19) changing to $\text{YBa}_2\text{Cu}_3\text{O}_7$ is $(80/650.19)16=1.969$ mg, [for $\text{NdBa}_2\text{Cu}_3\text{O}_y$, the change is $(80/705.48)16=1.8144$ mg because 705.48 is the formula weight of $\text{NdBa}_2\text{Cu}_3\text{O}_6$], which is much larger than the detection limit of 0.001 mg. This shows that the TGA method is one of the most powerful methods to study changes of oxygen content in $\text{RBa}_2\text{Cu}_3\text{O}_y$ compounds during heating or cooling in different atmospheres.

II.5. Electrical Measurements

Electrical conductivity was measured on cooling from 300 to 4 K using a standard four-probe method with In solder contacts at AT&T Bell Laboratories, Murray Hill, New Jersey.

It was found that rate of cooling affects the results of T_C measurement, i.e., the higher the rate of cooling, the lower the apparent T_C obtained. For example, for a sample of $\text{NdBa}_2\text{Cu}_3\text{O}_y$, its onset of T_C is 85 K at 20 K/min of cooling rate; but 89.6 K at 10 K/min. In order to eliminate the measurement error, a constant cooling rate (8 K/min) was maintained below 200 K for all samples tested.

III. RESULTS AND DISCUSSION

III.1. $\text{Y}_{1-x}\text{Bi}_x\text{Ba}_2\text{Cu}_3\text{O}_y$ System

The phase analysis by the x-ray diffraction powder method (Table 8.) shows that, in air, Bi^{3+} does not enter into the $\text{YBa}_2\text{Cu}_3\text{O}_y$ (Y-123, for short) structure since it is very easy for Y-123 and Ba_2BiYO_6 to form. However, the formation temperature of Y-123 is lower when Bi_2O_3 is present. These results are the same as those obtained by former researchers.[65,66,67]

Table 8. X-ray phase analysis in the $Y_{1-x}Bi_xBa_2Cu_3O_y$ system

x in $Y_{1-x}Bi_xBa_2Cu_3O_y$	Reaction conditions	Phase compositions					
		Y-123	BaBiY ^a	BaCuO ₂	BaCO ₃	CuO	Cu ₂ O
0	950°C, 16h, air	yes	no	no	no	no	no
0.1	940°C, 20h, air	yes	yes	? ^b	no	tr ^c	no
0	940°C, 7h, N ₂	?	no	no	yes	tr	yes
0.1	960°C, 7h, N ₂	?	yes	no	yes	no	tr
0.2	840°C, 7h, N ₂	?	yes	no	yes	?	?
0.2	940°C, 7h, N ₂	?	yes	no	yes	tr	tr
0	940°C, 7h, Ar	?	no	no	yes	tr	yes
0.2	940°C, 7h, Ar	?	yes	no	yes	tr	yes
0.2	930°C, 20h, Ar	?	yes	no	no	?	?

a: BaBiY means Ba₂BiYO₆.

b: ? means that it is uncertain whether the phase is present.

c: "tr" means that a trace of the phase was observed.

In inert atmosphere (N_2 or Ar), however, even on heating at higher temperatures and for longer times, Y-123 is still difficult to produce while some Ba_2BiYO_6 has already formed. The results (Table 8) show that the formation temperature of Ba_2BiYO_6 in N_2 is below $840^\circ C$. The formation of Ba_2BiYO_6 needs an oxidizing condition to increase the Bi oxidation state from $3+$ to $5+$. There are two possible reasons for Ba_2BiYO_6 to form in inert atmosphere: the first is the possibility of oxygen impurity in the inert gases; the second is that part of the Cu is reduced from $2+$ to $1+$ to provide the oxygen needed. The second reason can be proved from the experimental results shown in Table 8. i.e., in air, there is no Cu_2O present in samples either with or without Bi; in N_2 or Ar, however, there is Cu_2O , derived from reduction of CuO (or really Cu^{2+}), present in almost all samples. It should be pointed out that Parent et al^[80] also found that no $YBa_2Cu_3O_y$ phase could be obtained from preparations in inert atmosphere.

Noel et al ^[71] indicated that, of three $RBa_2Cu_3O_y$ systems, where $R = Y, Gd, \text{ or } Nd$, the Nd-Ba-Cu-O system is the most favorable for the formation of the R-123 superconductor because secondary phases are present in smaller quantities. It has also been mentioned before that $NdBa_2Cu_3O_y$ is isostructural with $YBa_2Cu_3O_y$ and has properties similar to those of $YBa_2Cu_3O_y$; also the difference in radii between Nd^{3+} and Bi^{3+} is only 5.4%. In order to continue the research-

ch on Bi-doping of $\text{RBa}_2\text{Cu}_3\text{O}_y$ in inert atmosphere, the Nd-Ba-Cu-O system was then chosen and focused upon.

III.2. $\text{Nd}_{1-x}\text{Bi}_x\text{Ba}_2\text{Cu}_3\text{O}_y$ System

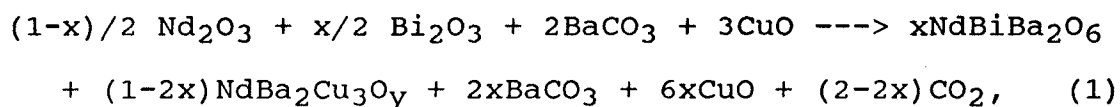
III.2.1. Preparations in air

It was found that $\text{NdBa}_2\text{Cu}_3\text{O}_y$ (Nd-123, for short) could be prepared by heating at $930-970^\circ\text{C}$ for 7-20 hours in air. By x-ray diffraction analyses, it was noted that, similarly to Y-123, a tetragonal Nd-123 would be obtained by fast cooling from the calcining temperature, and an orthorhombic Nd-123 obtained by slowly cooling in the furnace to room temperature (the photographs of x-ray patterns of these two types of Nd-123 are shown in APPENDIX II).

As in the Y-Bi-Ba-Cu-O system reported by other researchers,^[67] the calcined products in the Nd-Bi-Ba-Cu-O system displayed gradual color variation ranging from black to brown as the Bi addition increased.

As Table 9 shows, with Bi doping, a new minority phase is present at $x > 0.05$. The x-ray pattern of this new phase is similar to that of Ba_2BiYO_6 although there are some shifts between them since Nd^{3+} ($r=1.109$ A for CN=8) is larger than Y^{3+} ($r=1.019$ A for CN=8). Pure $\text{Ba}_2\text{BiNdO}_6$ was then synthesized and found to have an x-ray pattern identical with that of the new phase. Therefore the new phase is assumed to be $\text{Ba}_2\text{BiNdO}_6$ which has an isostructure of Ba_2BiYO_6 and a lattice constant, $a=8.703$ A (see APPENDIX II for the x-ray pattern of $\text{Ba}_2\text{BiNdO}_6$).

It was found that, as x increased, the amount of $\text{Ba}_2\text{Bi-NdO}_6$ also increased but there was no change in the lattice constants of Nd-123 as Bi-doping proceeded. This might mean that most of the Bi^{3+} ions do not enter into the lattice of Nd-123 and the maximum possible doping level is very low or even close to zero. Assuming all Bi^{3+} ions remain outside of Nd-123, the assumed reaction equation,



shows that some BaCO_3 and CuO should remain unreacted. In air or O_2 , at above 800°C , the remaining BaCO_3 and CuO may react to form BaCuO_2 ,^[81] which agrees with the results shown in Table 9.

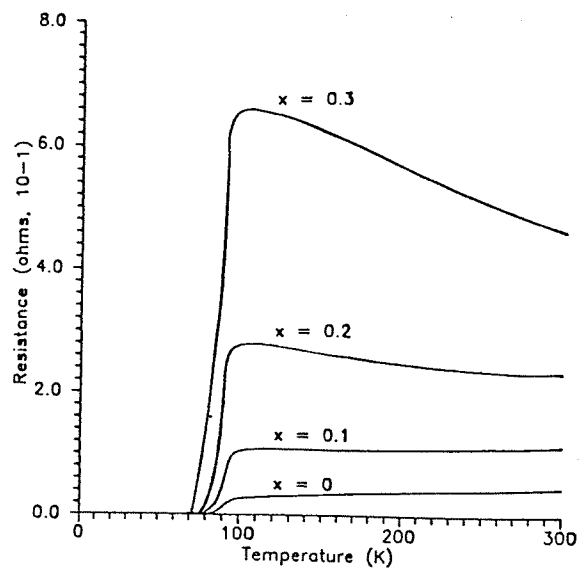
Table 9. X-ray analysis for $\text{Nd}_{1-x}\text{Bi}_x\text{Ba}_2\text{Cu}_3\text{O}_y$ prepared in air

		Phase compositions					
x in Nd_{1-x}	Reaction	-----					
$\text{Bi}_x\text{Ba}_2\text{Cu}_3\text{O}_y$	conditions	Nd-123	BaBiNd^a	BaCuO_2	BaCO_3	CuO	Cu_2O
0	$950^\circ\text{C}, 20\text{h}$	yes	no	no	no	no	no
0.1	$950^\circ\text{C}, 16\text{h}$	yes	yes	tr	no	tr	no
0.2	$800^\circ\text{C}, 14\text{h}$	no	yes	no	yes	yes	no
0.2	$950^\circ\text{C}, 6\text{h}$	yes	yes	yes	no	yes	no
1	$720^\circ\text{C}, 13\text{h}$	no	(BaBiO_3)	no	yes	yes	no

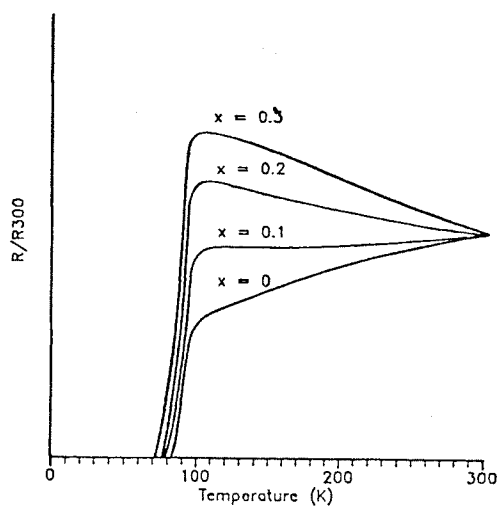
a: BaBiNd means $\text{Ba}_2\text{BiNdO}_6$.

As in $\text{YBa}_2\text{Cu}_3\text{O}_y$, the T_C of $\text{NdBa}_2\text{Cu}_3\text{O}_y$ also largely depends on the thermal history of the sample since this history will seriously affect oxygen content of the compound and thus the structure of the compound. The electrical measurements shown in Fig.17 (and also in Table 10) indicate that the normal resistivities of the samples with Bi doping are increased and the metallic behavior of pure Nd-123 is gradually changed to a semiconducting one as Bi replacement proceeds. At $x < 0.3$, the transition temperature range becomes broader as x increases though the onset of T_C is not obviously affected. These changes are caused by the presence of the non-superconducting phase, $\text{Ba}_2\text{BiNdO}_6$. At $x > 0.3$, the influence of $\text{Ba}_2\text{BiNdO}_6$ becomes larger as the relative amount of the phase increases, and T_C of the samples decreases while the transition range is even broader. The samples with nominally more than 50 mole % Bi [i.e. $\text{Bi}/(\text{Bi}+\text{Nd})100\%$] displayed no superconductivity at all. From the results obtained here, it can be concluded that there is a similarity between the Nd-Bi-Ba-Cu-O and Y-Bi-Ba-Cu-O systems in oxidizing atmosphere.

Yang et al^[82] found that, in the Y-Bi-Ba-Cu-O system, BaBiO_3 is formed at temperatures below 650°C ; the binary compound then reacted with Y_2O_3 to form Ba_2BiYO_6 at higher



(a)



(b)

Figure 17. Electrical resistance vs. temperature for nominal $\text{Nd}_{1-x}\text{Bi}_x\text{Ba}_2\text{Cu}_3\text{O}_y$ prepared in air and then annealed in O_2 at 400°C for 40 hours: (a) absolute resistance (note: e.g., 2.0 means 2.0×10^{-1} ohms); (b) R/R_{300} (R_{300} means the room temperature resistance of the samples). The onset, midpoint, and $R=0$ temperatures of transition are listed in Table 10.

Table 10. Onset, midpoint and $R = 0$ temperatures of
superconducting transition for nominal $\text{Nd}_{1-x}\text{Bi}_x\text{-Ba}_2\text{Cu}_3\text{O}_y$ made in air (Fig.17) or N_2 (Fig.18) and
annealed in air or O_2

x in compound	Transition temperature (K)		
	Onset	Midpoint*	$R = 0$

(see Fig.17)			
0	92	87	81
0.1	92	89	78
0.2	93	85	77
0.3	91	86	72

[see Fig.18 (a)]			
0	92	78	57
0.05	94	78	46
0.1	88	-	-
0.2	85	-	-
0.3	83	-	-
[see Fig.18 (b)]			
0.1 (curve 1)	70	-	26
0.1 (curve 2)	30	-	-

* Temperature at resistance midway between zero and the
resistance just prior to onset.

temperatures (700°C to 950°C); completion of Ba_2BiVO_6 formation is not realized until 950°C.

It should be pointed out that the x-ray diffraction patterns of BaBiO_3 and $\text{Ba}_2\text{BiNdO}_6$ are very similar to each other (see APPENDIX II) since the difference of ionic radii of Nd^{3+} and Bi^{3+} is very small (5.4%) as mentioned before. It was very hard to tell the two phases from each other by the x-ray method alone because of similarity of their x-ray patterns. However, under an optical transmission microscope, the BaBiO_3 and $\text{Ba}_2\text{BiNdO}_6$ made in inert atmosphere were observed to have different colors, blood-red and yellow-brown, respectively.

At 800°C, $\text{Ba}_2\text{BiNdO}_6$ (or BaBiO_3) was found to have formed in air while Nd-123 had not yet formed. On comparing the sample reacted at 930°C to one reacted at 950°C for the same period of time, 16 hours, it was also found that the ratio of Nd-123 to $\text{Ba}_2\text{BiNdO}_6$ in the latter was higher than that in the former. These results show that the formation of Nd-123 needs a higher temperature than that of the $\text{Ba}_2\text{BiNdO}_6$ phase. In other words, a higher temperature is more favorable for Nd-123 formation. The preparations of $\text{Nd}_{1-x}\text{Bi}_x\text{Ba}_2\text{Cu}_3\text{O}_y$ in inert atmosphere (N_2 or Ar) were, therefore, all carried out in such a way that the one-end-closed combustion tube containing the raw mixtures in the crucibles was put in the furnace after the reaction temperature, over the range 880-950°C, had been reached by the empty furnace.

III.2.2. Preparations in inert atmosphere

III.2.2.1 Reactions in inert atmosphere

It was found that all reactant mixtures with or without Bi were difficult to react completely in N_2 or Ar at the same calcining temperatures for the same period of time as in air. In other words, the completion of the reactions needed a much longer time if the same temperature as in air was used. A longer time instead of a higher temperature was adopted because it was found that the crystal grains of samples became very coarse and non-uniform at the high temperature; this is detrimental to the superconductivity of the products. The x-ray diffraction results of the samples are shown in Table 11.

X-ray patterns of the final sintered pellets indicate that Nd-123 formed in N_2 or Ar is not orthorhombic but tetragonal even if it was cooled very slowly in the furnace to room temperature in the inert atmosphere. This result is expected since in inert atmosphere there is not enough oxygen to provide for the structure transition from tetragonal to orthorhombic so that a tetragonal structure will be kept below the temperature of the T-O transition under oxidizing conditions. The x-ray pattern of Nd-123, rapidly cooled after preparation in inert atmosphere, was, however, a little different from that of the tetragonal Nd-123 made in air: some x-ray diffraction line doublets of the tetragonal Nd-123 became single lines, which may be caused by the deficiency of oxygen.

**Table 11. X-ray phase analysis for $\text{Nd}_{1-x}\text{Bi}_x\text{Ba}_2\text{Cu}_3\text{O}_y$
prepared in N_2**

		Phase compositions					
x in Nd_{1-x}	Reaction	-----					
$\text{Bi}_x\text{Ba}_2\text{Cu}_3\text{O}_y$	conditions	Nd-123	BaBiNd	BaCuO ₂	BaCO ₃	CuO	Cu ₂ O
0	920°C, 10h	yes	no	no	yes	yes	yes
0	950°C, 20h	yes	no	no	no	no	no
0.05	920°C, 20h	yes	?	no	no	no	?
0.1	920°C, 20h	yes	?	no	no	no	tr
0.2	940°C, 21h	yes	?	no	no	no	tr
0.3	920°C, 21h	yes	yes	no	no	no	yes
0.7	920°C, 20h	tr	yes	no	yes	yes	yes
0.9	920°C, 10h	?	yes	no	yes	tr	yes
1	900°C, 10h	no	(BaBiO ₃)	no	yes	yes	no
1	940°C, 10h	no	(BaBiO ₃)	no	yes	tr	yes

At $x < 0.2$, it was very difficult to find $\text{Ba}_2\text{BiNdO}_6$ in the x-ray patterns although there were some extra lines besides the lines of $\text{NdBa}_2\text{Cu}_3\text{O}_y$. This appeared to show that the inert atmosphere prevents this non-superconducting phase from forming. On careful study, the lattice constants of Nd-123 were found not to change as x increased from 0 to 0.3 or even higher. But as mentioned before, the size difference between Nd^{3+} and Bi^{3+} is very small and the x-ray patterns

showed little change when Nd^{3+} replaced part of the Bi^{3+} in BaBiO_3 . Therefore by the x-ray patterns alone, it is hard to say whether or not Bi^{3+} ions enter the Nd sites in Nd-123. It was noted, however, that some Cu_2O appeared in the x-ray patterns of the finally sintered samples. This result indirectly confirms that it is impossible for all Bi^{3+} ions to enter the Nd^{3+} sites even under the inert atmosphere conditions if one considers the stoichiometry of $\text{Nd}_{1-x}\text{Bi}_x\text{-Ba}_2\text{Cu}_3\text{O}_y$ (i.e., there should have been no Cu_2O remaining if all the Bi^{3+} had entered the Nd^{3+} sites.). Where are the Bi^{3+} ions if they are neither in $\text{Ba}_2\text{BiNdO}_6$ nor in Nd-123? The question will be answered later after presenting additional experimental results.

At $0.3 < x < 0.5$, in inert atmosphere, $\text{Ba}_2\text{BiNdO}_6$ obviously formed and coexisted with Nd-123. Trace quantities of Bi_2O_3 and Nd_2O_3 were also found in the sintered samples, which showed that the reactions are difficult to carry out completely in inert atmosphere. At $0.5 < x < 1$, not only did Nd-123 gradually disappear, but also $\text{Ba}_2\text{BiNdO}_6$ stopped forming unless Cu^{2+} was reduced to Cu^{1+} in order to provide oxygen for the formation of the latter.

From Equation (1) on page 55, it can be derived that, at $x > 0.25$, two compounds, $\text{NdBa}_2\text{Cu}_3\text{O}_6$ and $\text{Ba}_2\text{BiNdO}_6$ could not form at the same time if no oxygen is introduced from outside the system.

The number of oxygen atoms in the left side of the

equation =

$$1.5(1-x) + 1.5x + 6 + 3 = 10.5 \quad (i)$$

The number of oxygen atoms on the right side of the equation =

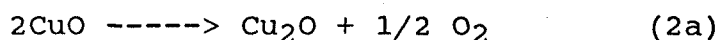
$$6x + (1-2x)y + 6x + 6x + 2(2-2x) \quad (ii)$$

If $y = 6$ and $(ii) > (i)$, we have,

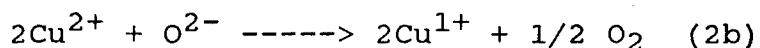
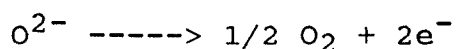
$$6x + (1-2x)6 + 6x + 6x + 2(2-2x) > 10.5,$$

$$x > 0.25.$$

However, our experimental results showed that both phases coexisted up to $x=0.5$; there are several reasons for this: i). oxygen impurity in N_2 or Ar used; ii). a little leakage from the open end of the combustion tube; and iii). perhaps the most important reason:

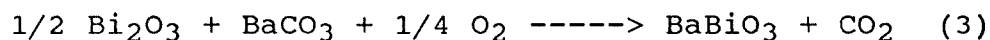


or actually because the Cu^{2+} may no longer be present as CuO:



In fact, Cu_2O was found even in the pure Nd-123 samples which reacted incompletely although Cu_2O finally disappeared when the reactions were totally finished (see Table 11). In the cases of Bi doping, however, Cu_2O could always be found even if the reactions were complete, or sometimes the reactions could not proceed further because there was not enough oxygen for the reactions to be completed. It was also noted

that there was no BaCuO_2 in the final products reacted in N_2 or Ar although this phase formed in air; instead, Cu_2O and BaCO_3 were found separately. This indicates that Cu_2O cannot react with BaCO_3 to form BaCuO_2 under non-oxidizing conditions, as is to be expected. The same situation applies to the formation of BaBiO_3 . At $x=1$, there was no BaBiO_3 formed in inert atmosphere if CuO did not change into Cu_2O and vice versa (see Table 10). In fact, the reaction equation,



shows that more oxygen must be provided beyond the two compounds to finish the reaction, because the Bi^{3+} must be oxidized to (at least an average of) Bi^{4+} . Therefore, part of "CuO" in nominal $\text{Nd}_{1-x}\text{Bi}_x\text{Ba}_2\text{Cu}_3\text{O}_y$ system becomes an oxygen source for the coexistence of $\text{NdBa}_2\text{Cu}_3\text{O}_6$ and $\text{Ba}_2\text{Bi-NdO}_6$ at $x > 0.25$ and the formation of BaBiO_3 at $x = 1$ in inert atmosphere.

Zhuang et al^[66] studied the nominal $\text{YBa}_2(\text{Cu}_{1-z}\text{Bi}_z)_3\text{O}_y$ ($z = 0$ to 0.9) system. Two phases, $\text{YBa}_2\text{Cu}_3\text{O}_y$ and Ba_2BiYO_6 were found when $z > 0.05$; and one more phase, CuO , was found when $z > 0.1$. With increasing Bi content, the content of $\text{YBa}_2\text{Cu}_3\text{O}_y$ decreased and that of Ba_2BiYO_6 increased at the same time. However, there were no changes in the lattice parameters of the two phases. It was concluded that the solid solubility of Bi in $\text{YBa}_2\text{Cu}_3\text{O}_y$ is small.

Two more systems, $\text{NdBa}_2\text{Cu}_{3-z}\text{Bi}_z\text{O}_y$ ($z < 0.15$) and $\text{Nd}_{1-x}\text{Bi}_x\text{Ba}_2\text{Cu}_{2.9}\text{Bi}_{0.1}\text{O}_y$ were therefore prepared in the current study in order to determine whether Bi could substitute

simultaneously or separately for Nd and Cu in $\text{NdBa}_2\text{Cu}_3\text{O}_y$ in inert atmosphere. Because of size (see Table 5), any Bi substituting for Nd is expected to be only Bi^{3+} while any Bi substituting for Cu is expected to be only Bi^{5+} . The x-ray diffraction results are shown in Table 12. It shows that, as Bi_2O_3 is added in quantities > 5 mole% [mole% here = $(\text{Bi}/(\text{Bi} + \text{Nd}))100$], multiphase systems result: besides Nd-123, $\text{Ba}_2\text{BiNdO}_6$, BaCO_3 , Cu_2O and trace Bi_2O_3 appeared in nominal $\text{NdBa}_2\text{Cu}_{3-z}\text{Bi}_z\text{O}_y$; and $\text{Ba}_2\text{BiNdO}_6$, BaCO_3 , trace CuO , Cu_2O , Bi_2O_3 and Nd_2O_3 in $\text{Nd}_{1-x}\text{Bi}_x\text{Ba}_2\text{Cu}_{2.9}\text{Bi}_{0.1}\text{O}_y$. There is no evidence that Bi enters either Nd or Cu sites in Nd-123 because in either case single phases should have appeared in the systems instead of the multiple phases.

Table 12. X-ray phase analysis for $\text{NdBa}_2\text{Cu}_{3-z}\text{Bi}_z\text{O}_y$ and $\text{Nd}_{1-x}\text{Bi}_x\text{Ba}_2\text{Cu}_{2.9}\text{Bi}_{0.1}\text{O}_y$ prepared in N_2

		Phase compositions						
x or z in Reaction	-----							
samples	conditions	Nd123	BaBiNd	BaCO_3	CuO	Cu_2O	Bi_2O_3	Nd_2O_3
z=0.05	930°C, 10h	yes	tr	yes	no	yes	tr	no
0.15	930°C, 10h	yes	tr	yes	no	yes	tr	no

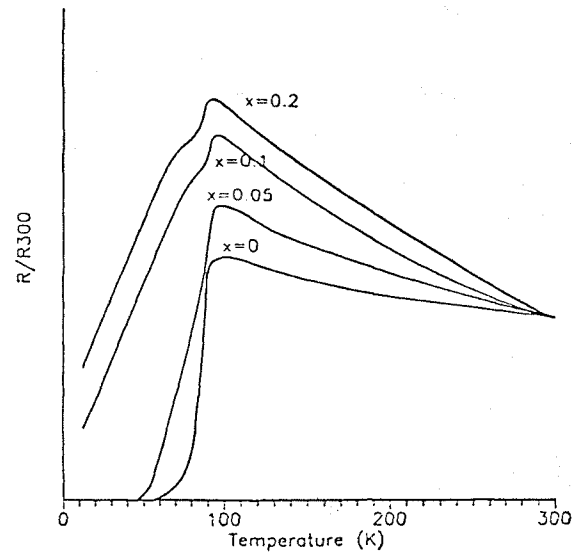
x=0.1	930°C, 10h	yes	tr	yes	no	yes	yes	yes
0.2	930°C, 10h	yes	tr	yes	no	yes	yes	yes
0.3	930°C, 10h	yes	yes	yes	tr	yes	yes	yes

III.2.2.2. Annealing to reintroduce oxygen

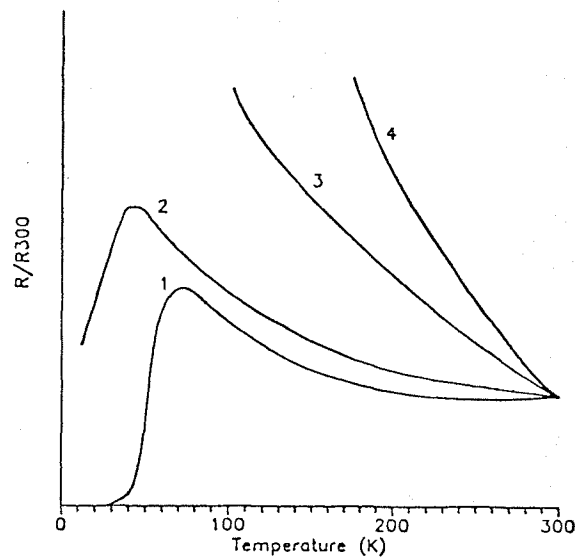
Due to the deficiency of oxygen, Nd-123 or possibly (Nd,Bi)-123 obtained in inert atmosphere is a tetragonal phase which exhibits no superconductivity. The finally-sintered discs at 880-950°C were annealed at 300-580°C in air or 250-480°C in O₂ (flow rate 31 cc/min) for periods of time ranging from several hours to several weeks in attempts to insert oxygen into the oxygen-deficient phases and obtain an orthorhombic superconducting phase. After annealing, the tetragonal Nd-123 was changed into the orthorhombic one, but at the same time, the cubic nonsuperconducting phase, Ba₂BiNdO₆, obviously appeared in the samples with less than 20 mole % Bi (x=0.2) down to 5 mole % Bi (x= 0.05) (see APPENDIX II). Judging from the relative changes of intensities of lines in the x-ray patterns of the samples, the amount of Ba₂BiNdO₆ depends on both the temperature and the time employed in annealing. The higher the temperature or the longer the time, the more Ba₂BiNdO₆ appeared. It was also found that, for a certain sample, the phase appearing during the annealing was always less than that obtained by directly reacting in air.

It was noted that, through annealing, there was a sample color change from grey to dark-brown while the intensity of the x-ray patterns of Ba₂BiNdO₆ changed from weak to strong.

The measurements of electrical conductivity (Fig.18) indicate that the superconductivity of the samples prepared in inert atmosphere is largely degraded even if the



(a)



(b)

Figure 18. Electrical resistivity vs. temperature for nominal $\text{Nd}_{1-x}\text{Bi}_x\text{Ba}_2\text{Cu}_3\text{O}_y$ prepared in N_2 and then annealed in air or O_2 : (a) all samples are annealed in O_2 at 480°C for 40 hours; (b) 1- $\text{Nd}_{0.9}\text{Bi}_{0.1}\text{Ba}_2\text{Cu}_3\text{O}_y$ annealed at 340°C in air for 20 hours and then in O_2 for 20 hours; 2- $\text{Nd}_{0.9}\text{Bi}_{0.1}\text{Ba}_2\text{Cu}_3\text{O}_y$ annealed at 340°C in air for 40 hours; 3- $\text{Nd}_{0.95}\text{Bi}_{0.05}\text{Ba}_2\text{Cu}_3\text{O}_y$ annealed at 300°C in air for more than one week; 4- $\text{Nd}_{0.8}\text{Bi}_{0.2}\text{Ba}_2\text{Cu}_3\text{O}_y$ annealed at 300°C in air for more than one week. The onset, mid-point, and $R=0$ temperatures of transition are listed in Table 10.

annealing process described is employed since it seems that a perfect orthorhombic Nd-123 is not easy to obtain from the oxygen-deficient Nd-123 in this way. There existed the double- T_C phenomenon [Fig.18(a)] mentioned on Page 26. T_C of a sample largely depended on the history of the sample [Fig.18(b)]. It has been reported^[83] that the T_C of Nd-123 is more sensitive to the oxygen content than Y-123. Therefore, for the Nd-123 made in inert atmosphere, a more effective method, e.g. plasma method^[31], might be needed if a maximum T_C is expected to be reached. However, the plasma method requires a long-time treatment except for thin films.

On comparing the results shown in Fig.18(a) and Fig.17(b), it can also be found that the T_C of the sample (with 30 mole % Bi) made in air is higher than the T_C of the sample (with 10 mole % Bi) made in inert gas. This indicates that the superconductivity of Nd-123 doped with Bi depends mainly on the degree of perfection of the Nd-123 phase instead of the amount of the non-superconducting phase, Ba_2BiNdO_6 , because the Nd-123 phase is actually in continuous physical contact in samples with small amounts of Bi ($0 < x < 0.3$).

III.2.2.3. Where are the Bi ions?

One of the original goals of this research was the substitution of Bi for Nd in Nd-123 in inert atmosphere. However, this does not seem to have been realized according to the experimental results obtained. For the samples made in inert atmosphere, although it is hard to find Ba_2BiNdO_6

or Bi_2O_3 in their x-ray patterns at $x < 0.2$, the presence of Cu_2O [it should also have trace BaCO_3 left at the same time according to Equation (1).] indicates that it is impossible for all Bi to enter the Nd sites as mentioned before. After annealing at a relatively low temperature in air or O_2 , $\text{Ba}_2\text{BiNdO}_6$ appears in the samples in which none of this phase was observed beforehand. Where are the Bi^{3+} ions before annealing? How is $\text{Ba}_2\text{BiNdO}_6$ produced at such low temperatures during annealing? These two questions should be answered if the possibility of substitution of Bi for Nd in Nd-123 is to be understood. The following experiments were designed to provide more information to answer these two questions.

Former researchers^[82] mentioned that Bi_2O_3 can react directly with prepared Y-123 to form $\text{Ba}_2\text{BiNdO}_6$ at temperatures as low as 800°C in air. Our results (Table 13) show that Bi_2O_3 has already reacted with prepared Nd-123 to form $\text{Ba}_2\text{BiNdO}_6$ at about 880°C in either air or inert atmosphere, N_2 or Ar. This means that Bi_2O_3 cannot exist unreacted above 880°C .

Another possibility is that Bi_2O_3 may not be detected by the x-ray diffraction powder method since the amount of Bi_2O_3 is relatively low (at $x = 0.2$, the Bi_2O_3 content is about 6 wt.%). In order to examine this possibility, mixtures of Nd-123 with 10 mole% and 20 mole% of Bi^{3+} were prepared.

Before reaction (that is, with physical mixtures only), Bi_2O_3 showed up clearly in the x-ray pattern of the mixture with 20 mole % Bi, although it was uncertain for the mixture with 10 mole % Bi. With reactions above 880°C in either air or N_2 , as Table 13 shows, the x-ray diffraction lines of Bi_2O_3 disappeared while those of $\text{Ba}_2\text{BiNdO}_6$ emerged. However, Bi_2O_3 still occurred unreacted after the mixture was heated at 550°C in air for more than 40 hours. These results show that Bi_2O_3 does react with some of the compounds included in this work at temperatures above 880°C even in N_2 so that no Bi_2O_3 remains after reaction. In other words, $\text{Ba}_2\text{BiNdO}_6$ appearing during annealing is not a product which might be formed by the reaction of Bi_2O_3 with the other compounds at annealing temperatures even below 400°C .

Table 13. X-ray phase analysis for products of reaction between Nd-123 and excess Bi_2O_3

		Phase compositions					
w in Nd-123	Reaction	-----					
w/2 Bi_2O_3	conditions	Nd-123	BaBiNd	BaCO_3	CuO	Cu_2O	Bi_2O_3
0.1	$550^\circ\text{C}, >40\text{h}, \text{air}$	yes	no	no	no	no	?
0.2	$550^\circ\text{C}, >40\text{h}, \text{air}$	yes	no	no	no	no	tr

0.1	$910^\circ\text{C}, 9\text{h}, \text{air}$	yes	yes	no	tr	no	no
0.1	$880^\circ\text{C}, 4\text{h}, \text{N}_2$	yes	tr	no	no	tr	no

Since no Bi_2O_3 remains after reaction at the high temperature ($\sim 900^\circ\text{C}$) even though $\text{Ba}_2\text{BiNdO}_6$ cannot be found in the x-ray patterns of the samples, is it possible for part of the Bi added in the nominal $\text{Nd}_{1-x}\text{Bi}_x\text{Ba}_2\text{Cu}_3\text{O}_y$ system to enter the Nd sites even though it has been concluded above that it is impossible for all the Bi to enter these sites? The answer is negative according to the experimental results described below.

By using an optical transmission microscope, it was found that a secondary phase with yellow-brown color appeared even though a small amount of Bi ($x > 0.05$) was introduced into the samples while the main phase, Nd-123, in either tetragonal or orthorhombic structure, was found to be black under the microscope. Oxygen-deficient BaBiO_3 and $\text{Ba}_2\text{BiNdO}_6$, which may be written as BaBiO_z ($z < 3$) and $\text{Ba}_2\text{BiNdO}_x$ ($x < 6$), were synthesized by reacting in inert atmosphere to determine the secondary phase. As mentioned before, under the microscope, the former is blood-red and the latter, yellow-brown. The secondary phase may therefore be identified as oxygen-deficient $\text{Ba}_2\text{BiNdO}_6$ or $\text{Ba}_2\text{BiNdO}_x$. By the way, both BaBiO_3 and $\text{Ba}_2\text{BiNdO}_6$ made in air are, like Nd-123, observed to be black under the microscope.

Thermogravimetric analysis was carried out for further confirmation that the $\text{Ba}_2\text{BiNdO}_x$ (oxygen-deficient $\text{Ba}_2\text{BiNdO}_6$) had been formed before annealing. The results are shown in Fig.19.

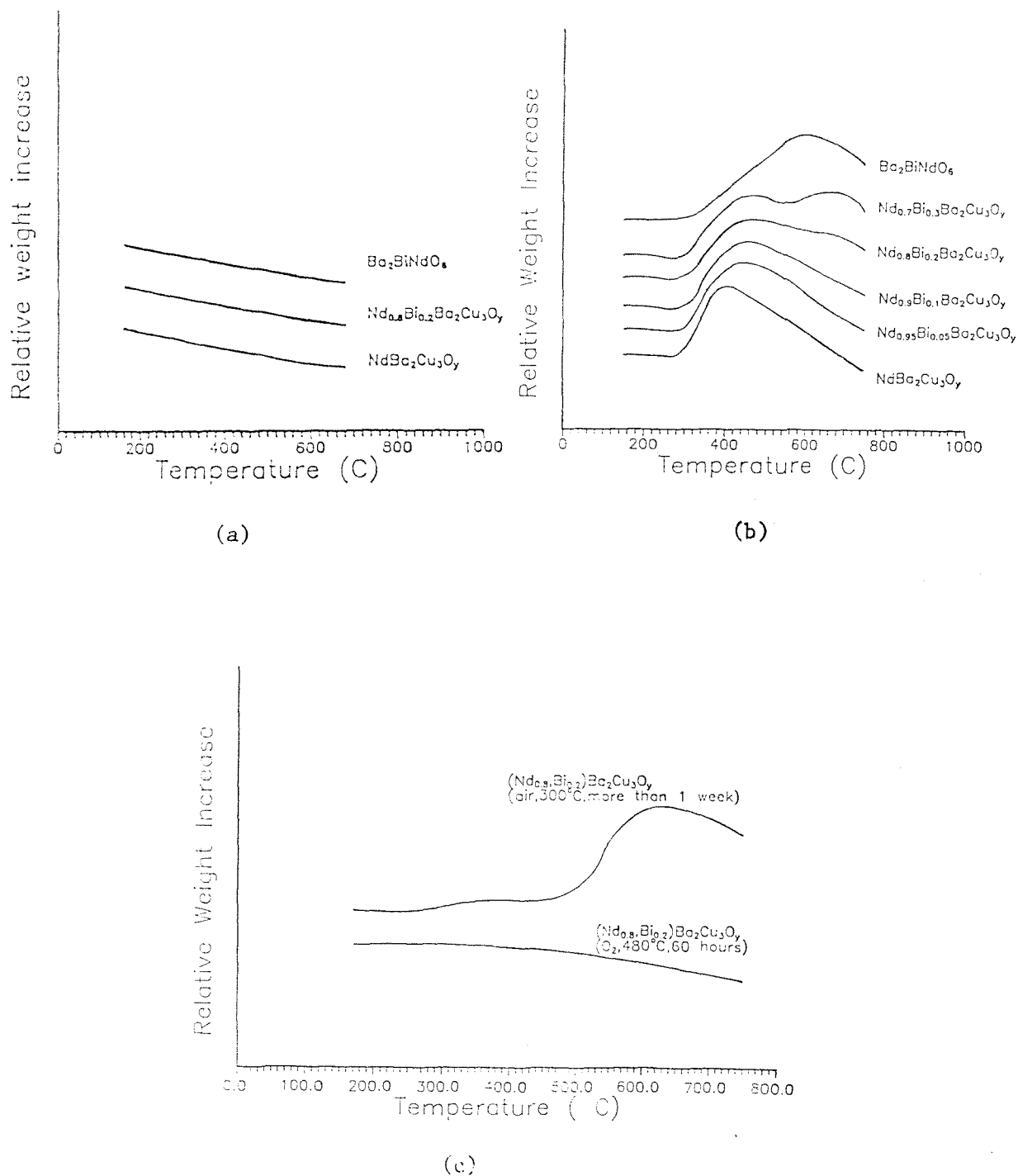


Figure 19. TGA results for nominal $\text{Nd}_{1-x}\text{Bi}_x\text{Ba}_2\text{Cu}_3\text{O}_y$ samples: (a) all samples prepared in air; (b) all samples prepared in N_2 ; (c) both samples prepared in N_2 and then annealed under the conditions indicated in the figure.

Table 14. Temperatures of TGA onset and maximum weight increase of the samples made in N₂ (TGA at rate of 40°C/min, in air)

Nominal compound	Onset (°C)	Maximum (°C)
NdBa ₂ Cu ₃ O _y	280	400
Nd _{0.95} Bi _{0.05} Ba ₂ Cu ₃ O _y	270	440
Nd _{0.9} Bi _{0.1} Ba ₂ Cu ₃ O _y	280	450
Nd _{0.8} Bi _{0.2} Ba ₂ Cu ₃ O _y	280	400, 560
Nd _{0.7} Bi _{0.3} Ba ₂ Cu ₃ O _y	300	400, 600
Ba ₂ BiNdO _x	305	570

For the samples prepared in air or prepared in N_2 but annealed above $300^{\circ}C$ in air or O_2 , the TGA traces showed no weight increase (and, in fact, a slight decrease) as the samples were reheated under oxidizing conditions (in air) in the TGA from room temperature up to $800^{\circ}C$ [Fig. 19 (a)]. This means that no detectable amount of oxygen is absorbed by these samples which have an orthorhombic structure confirmed by x-ray diffraction analysis mentioned above.

For the samples prepared in N_2 , however, their weights increased during heating in air in the TGA [Fig. 19 (b)]. The weight increases resulted from oxygen insertion. It was also found that different samples have different onset and maximum weight increase (or oxygen absorption) temperatures as shown in Table 14.

On comparison of the oxygen-deficient Nd-123 and Ba_2BiNdO_6 to the samples of $Nd_{1-x}Bi_xBa_2Cu_3O_y$ ($x = 0.05 - 0.3$), it is seen that the temperature of the maximum oxygen absorption shifts gradually from 400 to $570^{\circ}C$ as x increases from 0.05 to 0.3 while the temperatures of the maximum oxygen absorption of the pure Nd-123 and Ba_2BiNdO_x are found to be at about 400 and $570^{\circ}C$, respectively. This indicates that Ba_2BiNdO_x , an oxygen-deficient Ba_2BiNdO_6 phase, has already existed in the samples with Bi addition ($x > 0.05$) before being annealed, since the TGA traces of these samples are a superposition of at least two phases: the $NdBa_2Cu_3O_y$ and the Ba_2BiNdO_x prepared in inert atmosphere instead of one phase, the Nd-123. The Ba_2BiNdO_x phase made in inert

atmosphere, like the tetragonal Nd-123, absorbs more oxygen to improve or adjust its crystal structure when it is reheated in air at a relatively low temperature.

From the TGA results, it may also be concluded that, although the tetragonal Nd-123 has a lower temperature of maximum oxygen absorption than does the $\text{Ba}_2\text{BiNdO}_x$ made in inert atmosphere, it would not be likely to be able to reintroduce oxygen only into the tetragonal Nd-123 because both of them have almost the same temperature of onset of oxygen absorption (Table 14). In other words, being annealed above the onset temperatures of weight increase, the tetragonal Nd-123 will absorb more oxygen and gradually change to an orthorhombic structure; at the same time, however, the $\text{Ba}_2\text{BiNdO}_x$ phase coexisting with the Nd-123 will also absorb some oxygen to improve or adjust its structure although its maximum oxygen content ($x = 6$) may not be obtained if the annealing temperature is below its maximum weight increase temperature, e.g. 570°C (at rate of $40^\circ/\text{min}$ in air).

One example is shown in Fig.19(c); the nominal $\text{Nd}_{0.8}\text{-Bi}_{0.2}\text{Ba}_2\text{Cu}_3\text{O}_y$ sample, made in N_2 and then annealed in O_2 at 480°C for 60 hours, shows no weight increase or significant oxygen absorption during reheating in air in the TGA apparatus from room temperature to 800°C . However, the same type of sample but annealed in air at only 300°C for more than one week shows a weight increase or oxygen absorption during the TGA reheating. This means that, after the annealing process defined above, the former sample has already obtained

enough oxygen for the phases in it, both $\text{NdBa}_2\text{Cu}_3\text{O}_y$ and $\text{Ba}_2\text{BiNdO}_x$; the latter, however, has not yet got enough oxygen for both phases, especially the $\text{Ba}_2\text{BiNdO}_x$ which needs a higher temperature to obtain a maximum oxygen content compared to $\text{NdBa}_2\text{Cu}_3\text{O}_y$ as mentioned above.

According to the TGA results shown in Fig.19(b) and (c), it can also be seen that a lower annealing temperature is more favorable to make the Nd-123 with a higher oxygen content and the $\text{Ba}_2\text{BiNdO}_x$ with a lower oxygen content, i.e., vice versa. Therefore, by changing annealing temperatures, one may change the oxygen contents in both $\text{NdBa}_2\text{Cu}_3\text{O}_y$ and $\text{Ba}_2\text{BiNdO}_x$ in different directions, i.e., a higher oxygen content of $\text{NdBa}_2\text{Cu}_3\text{O}_y$ and a lower oxygen content of $\text{Ba}_2\text{BiNdO}_x$ may be obtained at a lower annealing temperature near the temperature corresponding to a maximum weight increase in $\text{NdBa}_2\text{Cu}_3\text{O}_y$; on the other hand, a lower oxygen content of $\text{NdBa}_2\text{Cu}_3\text{O}_y$ and a higher oxygen content of $\text{Ba}_2\text{BiNdO}_x$ may be realized at a higher annealing temperature near the temperature for a maximum weight increase in $\text{Ba}_2\text{BiNdO}_x$.

It should be pointed out that, although an optimum orthorhombic $\text{NdBa}_2\text{Cu}_3\text{O}_y$ might be formed while little oxygen has been inserted into the $\text{Ba}_2\text{BiNdO}_x$ by controlling annealing temperature, i.e. using a lower annealing temperature, there does not seem to be any possibility of obtaining a single phase $(\text{Nd,Bi})\text{Ba}_2\text{Cu}_3\text{O}_y$ compound in this way since the Bi has remained outside the Nd-123 but has already entered the $\text{Ba}_2\text{BiNdO}_x$ after high-temperature reaction in inert atmosphere

or before annealing in air or O_2 (this will be discussed further below). In other words, if the Bi doesn't enter the Nd-sites during reaction in inert atmosphere as our results show, it is not likely that the Bi enters the Nd-sites during annealing in an oxidizing atmosphere because, under an oxidizing condition, Bi^{3+} will more easily be oxidized to Bi^{5+} , which has a smaller size than Bi^{3+} (Table 5) and prefers to enter an oxygen octahedron (CN = 6) as the Bi in $BaBiO_3$ or Ba_2BiNdO_6 instead of an oxygen cube (CN = 8) as the Nd^{3+} in Nd-123. This means that the Ba_2BiNdO_6 phase and its effects on superconductivity cannot be eliminated by employing a more effective method, e.g. plasma method, than the thermal annealing used in our study even though the superconductivity of the samples with Bi made in inert atmosphere might be further improved because a complete formation of an optimum orthorhombic Nd-123 phase may be realized in this way.

Now that the oxygen-deficient Ba_2BiNdO_x has formed in inert atmosphere before annealing in air or O_2 , why is this phase difficult to recognize via x-ray diffraction? The x-ray pattern of the oxygen-deficient Ba_2BiNdO_6 made in inert atmosphere showed some differences from that of oxygen-normal Ba_2BiNdO_6 made in air (see APPENDIX II): for the former, i) the overall intensity is lower; ii) there are no diffraction lines at the large-angle area; and iii) the diffraction lines are generally broader and weaker. All these characteristics are those of a phase with a poor

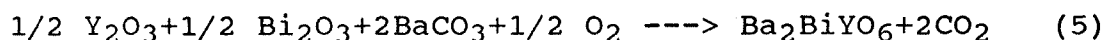
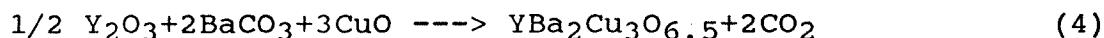
degree of crystallinity.^[84] Therefore, it is likely that a poorly crystallized intermediate phase precursor (we call it $\text{Ba}_2\text{BiNdO}_x$ above) of $\text{Ba}_2\text{BiNdO}_6$ was formed in inert atmosphere reaction before annealing in air or O_2 at a rather low temperature ranging from 300 to 500°C.

There are two reasons why the oxygen-deficient $\text{Ba}_2\text{BiNdO}_6$ is not easily detected by x-ray diffraction: first, its x-ray diffraction lines are too weak and broad; and secondly, its relative amount is very small. With the annealing proceeding in air or O_2 , however, the degree of crystallinity of the phase is gradually improved so that the x-ray diffraction intensities increase. Meanwhile, at $x > 0.3$, as the relative amount of the phase increases, its x-ray pattern strengthens. In both cases, the phase will become easier to observe and identify. With these points in mind, a trace of $\text{Ba}_2\text{BiNdO}_x$ (oxygen-deficient $\text{Ba}_2\text{BiNdO}_6$) phase was observed in the x-ray patterns of the samples with Bi less than 20 mole % ($x < 0.2$).

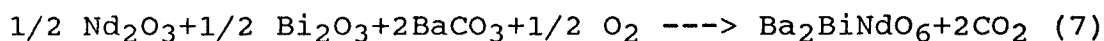
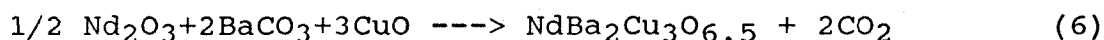
By using several methods including quantitative x-ray phase analysis and scanning electron microscopy (SEM), Zhuang et al^[66] claimed that it seems that there is a small amount of Bi dissolved in Y-123 phase. Like the Y-123 system, the possibility of trace substitution of Bi ($x < 0.05$) for Nd in Nd-123 may not be ruled out because of the limitations of the instrumentation employed. But it is believed that there would be a very small effect of such low replacement of Bi for Nd on the superconductivity of the Nd-

123 material as shown in the results obtained by the former researchers^[65,66,67] and this research.

If the possible trace substitution of Bi for Y or Nd in the 123 structure is neglected, for nominal $Y_{1-x}Bi_xBa_2Cu_3O_y$ system, there are actually two reactions:



Similarly, for the nominal $Nd_{1-x}Bi_xBa_2Cu_3O_y$ system, reactions are



Under oxidizing conditions, reactions (4) and (5) or (6) and (7) can be finished at the same time. In inert atmosphere, however, the reaction products are a result of competition between (4) and (5) or (6) and (7) because there is insufficient oxygen for both reactions to be completed. Our experiments show that, in inert atmosphere, under the reaction conditions employed, reaction (5) is easier to complete than reaction (4) so that Ba_2BiYO_6 results while $YBa_2Cu_3O_y$ has not yet formed; however, reactions (6) and (7) seem to have roughly the same reaction rates so that both Ba_2BiNdO_x and $NdBa_2Cu_3O_y$ result without normal (for the former) or maximum (for the latter) oxygen content.

In the inert atmosphere of either N_2 or Ar, Cu^{2+} is reduced to Cu^{1+} while the formation of Ba_2BiNdO_6 is also hindered. That is, the oxidation of Bi from Bi^{3+} to Bi^{5+} would be hindered. Even under this condition, however, it

seems to be very difficult for Bi^{3+} to enter the Nd sites in Nd-123, which indicates that the environment for Bi in BaBiO_3 or $\text{Ba}_2\text{BiNdO}_6$, in which Bi is surrounded by an oxygen octahedron, may be more favorable than that in Nd-123, in which Nd is surrounded by a distorted cube of oxygens. The differences of physical and chemical properties (e.g., ionic radius and electronegativity) between Nd^{3+} and Bi^{3+} may also contribute to the failure of Bi^{3+} to enter Nd-123.

It has therefore been found both by previous researchers and in the present study that Bi^{3+} ions do not enter into the rare earth sites in the 123 structure by simple solid-state reaction of Bi_2O_3 and Y_2O_3 or Nd_2O_3 , along with BaCO_3 and CuO in either oxidizing or inert atmosphere. However there might still be some possibility of such synthesis by the procedure employed for $\text{LaBa}_2\text{Cu}_3\text{O}_7$, which was mentioned above^[57]. That is, there might still be some possibility of obtaining (Y,Bi)-123 or (Nd,Bi)-123 by changing precursors of reactions so as to change the reaction procedure. With precursors other than those used in this study and, as a result, different reaction procedures, a mechanism for Bi to replace the rare earth in the 123 structure might result and thus (Y,Bi)-123 or (Nd,Bi)-123 may be obtained.

III.2.3. Preparations in reducing atmosphere

The x-ray patterns of preparations of $\text{Nd}_{1-x}\text{Bi}_x\text{Ba}_2\text{Cu}_3\text{O}_y$ in a reducing atmosphere (95 % Ar with 5% H_2) showed that

CuO in the samples was completely reduced to Cu metal so that the syntheses could not be carried out.

III.3 Some Other Systems

Besides $Y_{1-x}Bi_xBa_2Cu_2O_y$ and $Nd_{1-x}Bi_xBa_2Cu_3O_y$, substitutions for rare earth elements were attempted in some other systems:

III.3.1. $Y_{1-x}Tl_xBa_2Cu_3O_y$

Tl^{3+} has a radius similar to that of Y^{3+} and cannot be oxidized to Tl^{5+} (though Tl^+ also exists). Is there any possibility of Tl substitution for Y in Y-123? Samples were prepared in air at 910-950°C for 16-18 hours. The x-ray patterns of the finally-sintered samples indicated the presence of at least four phases, Y-123, Tl_2O_3 , CuO and $BaCO_3$. No changes were found in the Y-123 lattice constants as Tl doping proceeded. It can be concluded from the results that Tl does not enter the Y sites in Y-123. Ba_2TlYO_6 did not form in this case since Tl^{3+} cannot be oxidized to Tl^{5+} .

III.3.2. $La_{1.2-x}Bi_xBa_{1.8}Cu_3O_y$

A mixture of reactants designed to give the composition $La_{1.1}Bi_{0.1}Ba_{1.8}Cu_3O_y$ was heated at 940 °C in air for 20 hours. Four phases existed in the final product, La-123 (perhaps $La_{1.2}Ba_{1.8}Cu_3O_y$ rather than $LaBa_2Cu_3O_y$.^[39]), $BaCuO_2$, CuO, and Ba_2BiLaO_6 , which has an x-ray pattern similar to both Ba_2BiYO_6 and Ba_2BiNdO_6 and thus is isostructural

with these two compounds. The lattice constant of $\text{Ba}_2\text{BiLaO}_6$ has been determined in the current study to be $a = 8.77 \text{ \AA}$. This shows that this system is similar to the Y-Bi-Ba-Cu-O and Nd-Bi-Ba-Cu-O systems.

IV. CONCLUSIONS

The possibility of substitution of Bi and Tl for the rare earth elements Y and Nd (and also La) in the 123 superconductor structure in several reaction atmospheres has been investigated.

In inert atmosphere (N_2 or Ar), $\text{YBa}_2\text{Cu}_3\text{O}_y$ is very difficult to form while the non-superconducting Ba_2BiYO_6 phase still forms as it does in an oxidizing atmosphere (air or O_2); there is no evidence that any detectable (Y,Bi) $\text{Ba}_2\text{Cu}_3\text{O}_y$ compound forms.

Under oxidizing conditions, as in the Y-Bi-Ba-Cu-O system, both $\text{NdBa}_2\text{Cu}_3\text{O}_y$ and $\text{Ba}_2\text{BiNdO}_6$, which has a perovskite structure similar to Ba_2BiYO_6 and is also a non-superconducting phase, result simultaneously in the Nd-Bi-Ba-Cu-O system; there is no evidence for the formation of (Nd,Bi) $\text{Ba}_2\text{Cu}_3\text{O}_y$ in any detectable amount. The presence of the minority phase $\text{Ba}_2\text{BiNdO}_6$ in $\text{NdBa}_2\text{Cu}_3\text{O}_7$ samples results in a broader superconducting transition temperature and an increase in normal state resistivity.

In inert atmosphere (N_2 or Ar), $(Nd,Bi)Ba_2Cu_3O_y$ does not form to any detectable degree while formation of both the orthorhombic $NdBa_2Cu_3O_y$ and Ba_2BiNdO_6 is hindered since there is not enough oxygen to complete the reactions. A tetragonal $NdBa_2Cu_3O_y$ and an oxygen-deficient intermediate phase of Ba_2BiNdO_x result in the inert atmospheres. The oxygen-deficient Ba_2BiNdO_x is poorly crystallized and can be converted to a normal crystalline state by annealing in air or O_2 at a rather low temperature, that is, as low as $350^\circ C$. Superconductivity of the samples is severely deteriorated because the $NdBa_2Cu_3O_y$ phase formed in inert atmosphere is not easily changed by annealing in air or O_2 to an optimum orthorhombic structure, which is responsible for a high T_C in the 123 superconductors; meanwhile, there is an insulating minority phase, Ba_2BiNdO_6 , in the samples.

In reducing atmosphere (Ar with 5% H_2), CuO in the Nd-Bi-Ba-Cu-O system is completely reduced to Cu metal so that the syntheses cannot be carried out.

In air, Tl does not enter the Y sites in Y-123 and $Ba_2TlY_6O_{16}$ does not form because Tl^{3+} cannot be oxidized to Tl^{5+} .

In an oxidizing atmosphere, Ba_2BiLaO_6 is also found to be formed in the La-Bi-Ba-Cu-O system but no $(La,Bi)Ba_2Cu_3O_y$ appears. This means that, in oxidizing atmosphere, the La-Bi-Ba-Cu-O system is similar to the Y-Bi-Ba-Cu-O and Nd-Bi-Ba-Cu-O systems; i.e., Bi does not replace the Y or rare earth ions in the 123 structure but rather a nonsuperconducting perovskite phase, Ba_2BiRO_6 ($R = Y, Nd, \text{ and } La$), results.

REFERENCES

- 1 H.Kamerlingh Onnes, Akad.van Wetenschappen (Amsterdam)
14, 113, 818(1911).
- 2 C.Kittel, Introduction to Solid State Physics, 6th
edition, John Wiley & Sons, Inc.(1986), p.317-340.
- 3 J.Bardeen, L.N.Cooper, and J.R.Schrieffer, Phys.Rev.**106**,
162(1957); **108**, 1175(1957).
- 4 J.G.Bednorz and K.A.Muller, Z. Phys., B **64**, 189(1986).
- 5 R.J.Cava, A.Santoro, D.W.Johnson, W.W.Rhodes, Phys.Rev.B
35, 8770(1987).
- 6 M.K.Wu, J.R.Ashburn, C.J.Torng, P.H.Hor, R.L.Meng, L.Gao
Z.J.Huang, T.Q.Wang and C.W.Chu, Phys. Rev. Lett., **58**, 908
(1987).
- 7 J-M.Tarascon, W.R.McKinnon, L.H.Greene, G.W.Hull, and E.W.
Vogel, Phys. Rev. B **36**, 226(1987).
- 8 C.Michel, M.Hervieu, M.M.Borel, A.Grandin, F.Deslandes, J.
Provost, B.Raveau, Z. Phys. B: Condens. Matter., **68**, 421
(1987).
- 9 H.Maeda, Y.Tanaka, M.Fukutomi, T.Asano, Jpn. J. Appl.
Phys., **27**, L209(1988).
- 10 Z.Z.Sheng, A.M.Hermann, Nature, **332**, 55, 138(1988); Z.Z.
Sheng, A.M.Hermann, A.E.Ali, C.Almasan, J.Estrada,
T.Datta, Phys. Rev. Lett., **74**, 428(1988).
- 11 A.W.Sleight, M.A.Subramanian, and C.C.Torardi, MRS

- Bulletin, **14**(1), 45(1989).
- 12 I. K. Schuller and J.D.Jorgensen, MRS Bulletin, **14**(1) 27(1989).
- 13 R.J.Cava, B.Batlogg, J.J.Krajewski, L.W.Rupp, L.F.Schneemeyer, T.Siegrist, R.B.vanDover, P.Marsh, W.F.Peck,Jr, P.K.Gallagher, S.H.Glarum, J.H.Marshall, R.C.Farrow, J.V.Waszcak, R.Hull, and P.Trevor, Nature, **336**, 211(1988).
- 14 R.J.Cava, Science, **247**, 656(1990).
- 15 R.J.Cava, B.Batlogg, J.J.Krajewski, R.Farrow, L.W.Rupp, Jr., A.E.White, K.Short, W.F.Peck, and T.Kometani, Nature, **333**, 814(1988).
- 16 L.F.Schneemeyer, J.K.Thomas, T.Siegrist, B.Batlogg, L.W. Rupp, R.L.Opila, R.J.Cava, and D.W.Murphy, Nature, **335**, 421(1988).
- 17 L.Suchow, in Solid State Chemistry and Physics: An Introduction, edited by P.F. Weller. Vol.1, p.123(1973 -1974); M.Dekker, New York.
- 18 J.F.Schooley and W.R.Thurber, J. Phys. Soc. Jap., Suppl.**21**, 639(1966).
- 19 M.D.Banus, T.B.Reed, A.J.Strauss, Phys. Rev. B **5**(8), 2775(1972).
- 20 D.C.Johnston, H.Prakash, W.H.Zachariasen, R.Viswanathan, Mater. Res. Bull. **8**(7), 777(1973).
- 21 A.W.Sleight, J.L.Gillson, and P.E.Bierstedt, Solid State Commun., **17**(1), 27(1975).
- 22 D.E.Cox and A.W.Sleight, Proc. Conf. Neutron Scattering,

- 1, 45-54(1976).
- 23 C.Chaillout, A.Santoro, J.P.Remeika, A.S.Cooper, G.P. Espinosa, and M.Marezio, Solid State Commun., **65**, 1363 (1988).
- 24 S.Tajima, S.Uchida, A.Masaki, H.Takagi, K.Kitazawa, S. Tanaka, and S.Sagai, Phys. Rev. **B35**, 696(1987).
- 25 D.C.Hinks, B.Dabrowski, J.D.Jorgensen, A.W.Mitchell, D.R. Richards, S. Pei, and D. Shi, Nature, **333**, 836(1988).
- 26 See J.D.Jorgensen, Jpn. J. Appl. Phys. 26(Supplement 26-3), 2017(1987) for a review of the relevant literature.
- 27 M.A.Beno, L.Soderholm, D.W.Capone II, D.G.Hinks, J.D.Jorgensen, J.D.Grace, I.K.Schuller, C.U.Seger, and K.Zhang, Appl. Phys. Lett. **51**, 57(1987).
- 28 C.N.Rao and B.Raveau, Acc. Chem. Res., **22**(3), 106(1989).
- 29 A.M.Kini, U.Geiser, H.C.I.Kao, K.D.Carlson, H.H.Wang, M.R. Monaghan, and J.M.Williams, Inorg. Chem., **26**, 1834 (1987).
- 30 J-M.Tarascon and B.G.Bagley, MRS Bulletin, **14**(1), 53 (1989).
- 31 B.G.Bagley, L.H.Greene, J-M.Tarascon, and G.W.Hull, Appl.Phys.Lett. **51**(8), 622(1987).
- 32 J.D.Jorgensen, M.A.Beno, D.G.Hinks, L.Soderholm, K.J.Volin, R.L.Hitterman, J.D.Grace, I.K.Schuller, C.U.Segre, K.Zhang, and M.S.Kleefisch, Phys.Rev. **B 36**, 3608(1987).
- 33 J-M.Tarascon, P.Barboux, B.G.Bagley, L.H.Greene, W.R.McKinnon, and G.W.Hull, in Chemistry of High

- Temperature Superconductors, edited by D.L.Nelson, M.S.Whittingham, and T.F.George (American Chemical Society, Washington, DC, 1987), p.198.
- 34 R.J.Cava, B.Batlogg, C.H.Chen, E.A.Rietman, S.M.Zahurak, and D.Werder, *Nature*, **329**, 423(1987).
 - 35 R.J.Cava, B.Batlogg, S.A.Sunshine, T.Siegrist, R.M. Fleming, K.Rabe, L.F.Schneemeyer, D.W.Murphy, R.B.van Dover, P.K.Gallagher, S.H.Glarum, S.Nakahara, R.C.Farrow, J.J.Krajewski, S.M.Zahurak, J.V.Waszczaek, J.H.Marshall, P.Marsh, L.W.Rupp,Jr., W.F.Peck and E.A.Rietman, *Physica C* **153-155**, 560(1988).
 - 36 J-M.Tarascon, W.R.McKinnon, L.H.Greene, G.W.Hull, B.G.Bagley, E.M.Vogel, and Y.LePage, in *High Temperature Supercon-11*, Pittsburgh, PA, 65(1987).
 - 37 B.G.Bagley, L.H.Greene, J-M.Tarascon, and G.W.Hull, *Applied Phys.Lett.* **51**, 622(1987).
 - 38 M.Alario-Franco and C.Chailout, *Physica C* **153-155**, 956(1988).
 - 39 See J.T.Markert, B.D.Dunlap, and M.B.Maple, *MRS Bulletin*, **14**(1), 41-42(1989), for a review of the relevant literature.
 - 40 L.Suchow, J.R.Adam, and K.S.Sohn, *J. Superconductivity*, **2**(4), 485(1989).
 - 41 B.W.Veal, W.K.Kwok, A.Umezawa, G.W.Crabtree, J.D. Jorgensen, J.W.Downey, L.J.Nowicki, A.W.Mitchell, A.P.Paulikas, and C.H.Sowers, *Appl. Phys. Lett.*, **51**(4), 279(1987).

- 42 Y.Tokura, J.B.Torrance, T.C.Huang, and A.I.Nazzal, Phys. Rev. B **38**, 7156(1988).
- 43 A.Tokiwa, Y.Syono, M.Kikuchi, R.Suzuki, T.Kajitani, N.Kobayashi, T.Sasaki, O.Nakatsu, and Y.Muto, Jpn.J.Appl. Phys, **27**, L1009(1988).
- 44 R.J.Cava, B.Batlogg, R.M.Fleming, S.A.Sunshine, A.Ramirez, E.A.Rietman, S.M.Zahurak, and R.B.van Dover, Phys. Rev. B **37**, 5912(1988).
- 45 R.Liang, Y.Inaguma, Y.Takagi, and T.Nakamura, Jpn. J. Appl. Phys. **26**, 1150(1987).
- 46 P.Somasundaram, K.S.Nanjundaswamy, A.M.Umarji, C.N.R.Rao, Mater. Res. Bull. **23**, 1139(1988).
- 47 M.Kosuge, B.Okai, K.Takahashi, and M.Ohta, Jpn. J. Appl. Phys. **27**, L1022(1988).
- 48 Y.Dalichaouch, M.S.Tarikachvili, E.A.Early. B.W.Lee, C.L.Seaman, K.N.Yang, H.Zhou, and M.B.Maple, Solid State Commun. **65**, 1001(1988).
- 49 C.Dong, J.K.Liang, G.C.Che, S.S.Xie, Z.X.Zhao, Q.S.Yang, Y.M.Ni, and G.R.Liu, Phys. Rev. B **37**, 5182(1988).
- 50 A.Maeda, T.Yabe, K.Uchinokura, and S.Tanaka, Jpn. J. Appl. Phys. **26**, L1368(1988).
- 51 Y.Song, J.P.Golben, S.Chittipeddi, J.R.Gaines, and A.J.Epstein, Phys. Rev. B **38**, 4605(1988).
- 52 Y.Song, J.P.Golben, X.D.Chen, J.R.Gaines, M-S.Wong, and E.R.Kreidler, Phys. Rev. B **38**, 2858(1988).
- 53 A.Maeda, T.Yabe, K.Uchinokura, M.Izumi, and S.Tonaka, Jpn. J. Appl. Phys. **26**, L1550(1988).

- 54 S.I.Lee, J.P.Golben, S.Y.Lee, X.D.Chen, Y.Song, T.W.Noh,
R.D.McMichael, J.R.Gaines, D.L.Cox, and B.R.Patton, Phys.
Rev. **B 36**, 2417(1988).
- 55 R.L.Meng, P.H.Hor, Y.Q.Wang, Z.J.Juang, Y.Y.Sun, L.Gao,
J. Betchold, and J.C.Chu, Extended Abstracts High
Temperature Superconductors **II**, Reno, NV, p. 233-235,
April 1988.
- 56 T.Wada, N.Suzuki, T.Maeda, S.Uchida, K.Uchinakura, and S.
Tanaka, Appl. Phys. Lett. **52**, 1989(1988).
- 57 M.H.Ghandehari and S.G.Brass, J.Mater.Res. **4**,
1111(1989).
- 58 S.Jin, R.C.Sherwood, R.B.van Dover, T.H.Tiefel, and D.W.
Johnson, Appl. Phys. Lett. **51**, 203(1987).
- 59 D.W.Murphy, S.Sunshine, R.B.van Dover, R.J.Cava, B.Bat-
logg, S.E.Zahurak, and L.F.Schneemeyer, Phys. Rev. Lett.
58, 1888(1987).
- 60 P.Chaudhari, R.H.Koch, R.B.Laibowitz, and R.J.Gambino,
Phys. Rev. Lett. **58**, 2684(1987).
- 61 B.Oh, M.Naito, S.Arnason, P.Rosenthal, R.Barton,
M.R.Beasley, T.H.Geballe, R.H.Hammond, and A.Kapitulnik,
Appl. Phys. Lett. **51**, 852(1987).
- 62 S.H.Kilcoyne and R.Cywinski, J.Phys.**D20**, 1327(1987).
- 63 L.Chaffron, J.P.Mercurio and B.Frit, Ind. Ceram. (Paris)
835, 122-124(1989).
- 64 J.Jung, J.P.Franck, W.A.Milner and M.A-K.Mohamed, Phys.
Rev. **B37**, 3510(1988).
- 65 S.K.Blower and C.Greaves, Solid State Commun. **68**(8), 765

- (1988).
- 66 J.Zhuang, W.Su, H.Liu, Y.Wang, and J.Zhou, J. Less-Common Metals, **149**, 427-434(1989).
 - 67 N.Yang, R.S.Liu, W.N.Wang, Y.H.Chao, H.C.Lin, and P.T.Wu Physica **C 162-164**, 71-72(1989).
 - 68 N.D.Spencer and A.L.Roe, in Chemistry of High-Temperature Superconductors II, edited by D.L.Nelson and T.F.George, American Chemical Society, Washington, DC (1988), p.145.
 - 69 R.D.Shannon, Acta Cryst., **A32**, 751(1976).
 - 70 W.D.Arnett, D.R.Zint, C.E.Hamrin, Jr., R.J.De Angelis, K.Okazaki, D.K.Kim, X.X.Ding, W.D.Ehmann, J.W.Brill, T.N.O'Neal, L.E.DeLong, M.S.Osofsky, V.Le Tourneau, and S.A. Wolf, J. Superconductivity, **1**, 427(1988).
 - 71 D.Noel and L.Parent, Thermochim. Acta, **147**(1), 109(1989).
 - 72 Q.G.Luo and R.Y.Wang, J. Phys. Chem. Solids, **48**, 425 (1987).
 - 73 R.Asokamani and R.Manjula, Phys. Rev. **B39**, 4219(1989).
 - 74 S.Ichikawa, J. Phys. Chem. Solids, **50**, 931(1989).
 - 75 S.Ichikawa, J. Phys. Chem., **93**(21), 7320(1989).
 - 76 D.A.Nepela and J.M.McKay, Physica **C 158**, 65(1989).
 - 77 L.Pauling, The Nature of the Chemical Bond, 3rd edition p.93, Cornell University Press, Ithaca, New York (1960).
 - 78 W.Gordy, Phys. Rev. **69**, 604(1946).
 - 79 R.C.Weast and M.J.Astle, CRC Handbook of Chemistry and Physics, 59th edition(1978-1979).
 - 80 L.Parent, B.Champagne, K.Cole and C.Moreau, Supercond. Sci. Technol., **2**(2), 103-106(1989).

- 81 H.Migeon, F.Jeannot, M.Zanne and J.Aubryal, Rev. Chim. Miner., **13**, 440(1976).
- 82 N.Yang, R.S.Liu, W.N.Wang and P.T.Wu, "Effects of Bi Replacement for Cu upon the Microstruture and Superconductivity of $\text{YBa}_2\text{Cu}_3\text{O}_y$ ". Private communication from authors, who claimed to have submitted this to J. Mater. Sci., 1989.
- 83 B.W.Veal, A.P.Paulikas, J.W.Downey, H.Claus, K.Vandervoort, G.Tomlins, H.Shi, M.Jensen, and L.Morss, Physica C **162-164**, 97(1989).
- 84 H.Lipson, Interpretation of X-ray powder diffraction patterns, edited by H.Lipson and H.Steeple. London, Macmillan; New York, St.Martin's Press(1970), p.247.

APPENDIX I *

5-0574 MINOR CORRECTION

d	3.06	1.87	1.60	4.34	Y ₂ O ₃ ★					
I/I ₁	100	46	31	16	Yttrium ^{III} Oxide					
Rad. Cu	λ 1.5405		Filter Ni		d Å	I/I ₁	hkl	d Å	I/I ₁	hkl
Dia.	Cut off		Coll.		4.34	16	211	1.443	3	721
I/I ₁ G.C. DIFFRACTOMETER	d corr. abs.?		d corr. abs.?		3.060	100	222	1.417	2	642
Ref. SWANSON AND FUYAT, NES CIRCULAR 539, VOL. ^{III} (1953)					2.652	30	400	1.346	2	732
Sys. CUBIC (BODY-CENTERED)	S.G. T ^B - I ₂ ,3				2.500	7	411	1.325	4	800
a ₀ 10.604 b ₀ c ₀	A C				2.372	1	420	1.305	3	811
α β γ	Z 16				2.261	8	332	1.287	1	820
Ref. ^{IBID.}					2.165	1	422	1.267	2	653
ε n _D 1.77 ε _γ	Sign				2.080	12	510	1.249	1	822
2V D ₅ 657 mp	Color				1.936	3	521	1.233	3	831
Ref.					1.874	46	440	1.216	8	662
SAMPLE FROM THE NES SPEC. LAB. SPECT. ANAL. I					1.818	2	530	1.1854	5	840
<0.1% Ba; <0.01% Ca, Er, Si; <0.001% Mg, Pb, Yb.					1.769	<1	600	1.1708	1	910
X-RAY PATTERN AT 27°C.					1.720	5	611	1.1570	1	842
REPLACES 1-0831					1.677	1	620	1.1436	2	921
					1.636	4	541	1.1178	2	930
					1.599	31	622	1.0939	2	932
					1.563	7	631	1.0821	5	844
					1.531	5	644	1.0711	2	941
					1.499	2	710	1.0606	1	10.0.0
					1.470	1	640	1.0499	<1	10.1.1

1966

5-0378 MINOR CORRECTION

d	3.72	3.68	2.15	4.56	BaCO ₃ ★					
I/I ₁	100	53	28	9	Barium Carbonate (WITHERITE)					
Rad. Cu	λ 1.5405		Filter Ni		d Å	I/I ₁	hkl	d Å	I/I ₁	hkl
Dia.	Cut off		Coll.		4.56	9	110	1.706	1	240
I/I ₁ G.C. DIFFRACTOMETER	d corr. abs.?		d corr. abs.?		4.45	4	020	1.677	5	311
Ref. SWANSON AND FUYAT, NES CIRCULAR 539, VOL. ^{III} (1953)					3.72	100	111	1.649	4	133, 241
Sys. ORTHORHOMBIC	S.G. D _{2h} ¹⁶ - P6 ₃ CM				3.68	53	021	1.633	4	151
a ₀ 5.314 b ₀ 8.904 c ₀ 6.430	A 0.597 C 0.722				3.215	15	002	1.563	3	223
α β γ	Z 4				3.025	4	012	1.543	<1	043
Ref. ^{IBID.}					2.749	3	102	1.521	4	330
ε n _D 1.530	n _D 1.679 ε _γ 1.680		Sign -		2.656	11	200	1.508	2	242
2V D ₄ 308 mp	Color				2.628	24	112	1.484	1	060, 143
Ref. ^{IBID.}					2.590	23	130	1.375	6	332, 204
SAMPLE FROM MALLINCKRODT CHEM. WORKS. SPECT. ANAL. I					2.281	6	220	1.366	4	134
<0.01% Al, Ca, Na, Sr; <0.001% Cu, Fe, Mg, Pb.					2.226	2	040	1.348	4	313, 062
X-RAY PATTERN AT 26°C.					2.150	28	221	1.335	3	243
REPLACES 1-0506, 2-0364					2.104	12	041	1.328	4	400, 153
					2.048	10	202	1.295	3	260
					2.019	21	132	1.248	1	234, 421
					1.940	15	113	1.215	<1	071
					1.859	3	222	1.233	2	025, 351
					1.830	2	042	1.215	<1	253, 412
					1.737	2	310, 032	1.215	<1	171

1879

* All the cards shown here and below come from: The Powder Diffraction File (1964), ASTM special technical publication 48-N2, published by the American Society for Testing and Materials.

5-0661 MINOR CORRECTION

d	2.52	2.32	2.53	2.751	CuO					
I/I ₁	100	96	49	12	COPPER(II) OXIDE (TENORITE)					
Rad. CuKα ₁ λ 1.5405 Filter Ni Dia. Cut off Coll. d corr. abs. 7					d Å	I/I ₁	hkl	d Å	I/I ₁	hkl
Ref. SWANSON AND TATGE, NBS CIRCULAR 539, Vol. 1, 1953					2.751	12	110	1.1697	5	313
S.G. MONOCLINIC S.G. C _{2h} - C2/c					2.530	49	002	1.1620	3	222
a 4.684 b 3.425 c 5.129 A 1.368 C 1.498					2.523	100	111	1.1585	2	312
β 99°28' γ Z 4					2.323	96	111	1.1556	4	400
Ref. IBID.					2.312	30	200	1.1233	2	402, 223
ε a n _D β ε γ Sign					1.959	3	112	1.0916	6	131
2V Dx 6.51 mp Color					1.866	25	202	1.0737	2	131
Ref.					1.778	2	112	1.0394	<1	204
SAMPLE FROM JOHNSON MATTHEY AND CO. SPECT.					1.714	8	020	1.0178	3	024, 223
ANAL.: FAINT TRACES OF FE AND MG.					1.581	14	202	1.0074	4	313
X-RAY PATTERN AT 26°C					1.505	20	113	0.9921	<1	402
					1.418	12	022	.9808	4	224, 115
					1.410	15	311, 310	.9576	3	420
					1.275	19	220, 113	.9435	<1	133
					1.304	7	311, 312	.9390	4	122
							221	.9332	2	204
					1.265	6	004	.9209	2	115, 331
					1.262	7	222	.9100	2	133
REPLACES 1-1117, 2-1040, 2-1041, 3-0867, 3-0884					1.1961	2	204, 114	.9039	1	511

2026

14-699

d	3.25	2.69	2.71	5.28	α-Bi ₂ O ₃					
I/I ₁	100	45	40	2	ALPHA BISMUTH(III) OXIDE (BISMITE)					
Rad. CuKα ₁ λ 1.5405 Filter Ni Dia. Cut off I/I ₁ DIFFRACTOMETER					d Å	I/I ₁	hkl	d Å	I/I ₁	hkl
Ref. NAT. BUREAU OF STANDARDS (U.S.) MONO. 25 SEC. 3 1963					5.276	2	012	2.154	6	214
S.G. PSEUDORHOMBIC S.G. P2 ₁ /c (14) *					4.498	4	111	2.138	2	034
a 5.850 b 8.166 c 13.827 A 0.5906 C 0.4231					4.084	4	020	2.132	8	125
α β γ Z 8 Dx 9.370					3.622	8	103	2.041	2	040
Ref. IBID.					3.517	2	022	2.0064	6	026
ε a n _D β ε γ Sign					3.456	20	004	1.9922	4	230
2V D mp Color LIGHT YELLOW					3.310	35	113	1.9584	25	224, 042
Prepared from sample of bismuth trioxide obtained from Johnson, Matthey and Co., Ltd. Spec. analysis: less than 0.001% each of Si, Al, Pb, Ag and Na. Pattern made at 25°C.					3.253	100	121	1.9317	<1	301
* MONOCLINIC CELL HAS a=5.85, b=8.166, c=7.51, β=112°56.5					3.184	25	014	1.9136	2	232
Z=4					2.753	4	210	1.9098	4	141
					2.708	40	123	1.8787	10	311
					2.693	40	202	1.8720	18	107
					2.638	4	024	1.8409	6	135
					2.557	14	212	1.8237	8	117
					2.532	10	032	1.8087	1	204
					2.499	8	106	1.7967	<1	303
					2.429	6	131	1.7790	2	143
					2.390	14	115	1.7660	8	216
					2.244	6	222	1.7590	10	036
					2.176	6	133	1.7414	1	311

PLUS 27 LINES TO 1.34 Å²

5-0667 MINOR CORRECTION

d	2.47	2.14	1.51	3.020	Cu ₂ O					
I/I ₁	100	37	27	9	COPPER (I) OXIDE (CUPRITE)					
Rad. CuK α_1	λ 1.5405	Filter Ni			d Å	I/I ₁	hkl	d Å	I/I ₁	hkl
Dia. Cut off		Coll.			3.020	9	110			
I/I ₁ G. C. DIFFRACTOMETER	d corr. abs.?				2.465	100	111			
Ref. SWANSON AND FUYAT, NBS CIRCULAR 539, Vol. II					2.135	37	200			
					1.743	1	211			
					1.510	27	220			
Sym. CUBIC		S.G. O _h - Pn3m			1.287	17	311			
a ₀ 4.2696 b ₀	c ₀	A	C		1.233	4	222			
α	β	γ	Z 2		1.0674	2	400			
Ref. ibid.					0.9795	4	331			
ϵ a	n ω β	ϵ γ	Sign		.9548	3	420			
2V	D _x 100 mp	Color			.8715	3	422			
Ref.					.8216	3	511			
SAMPLE PREPARED AT THE NBS. SPECT. ANAL. 1.4% Ca, Si; <0.1% Al, Mg; <0.01% Ag, B, Ba, Fe, Ti; <0.001% Mn, Pb, Sn.										
X-RAY PATTERN AT 26°C.										
REPLACES 1-1142, 2-1067, 3-0892, 3-0898										

2031

6-0408

d	2.90	2.32	1.92	3.32	Nd ₂ O ₃					
I/I ₁	100	35	25	35	NEODYMIUM OXIDE					
Rad. Cu	λ 1.5405	Filter			d Å	I/I ₁	hkl	d Å	I/I ₁	hkl
Dia. Cut off		Coll.			3.319	35	100	1.0627	11	213
I/I ₁	d corr. abs.?				2.998	32	002	1.0375	8	202
Ref. SWANSON ET AL., NBS CIRCULAR 539, Vol. II					2.902	100	101	0.9721	7	205
					2.725	33	102	.9621	6	214
					1.916	35	110	.9574	5	106
Sym. HEXAGONAL		S.G. D _{3h} - P321			1.713	31	103	.9203	2	210
a ₀ 3.831 b ₀	c ₀ 5.999	A	C		1.659	6	200	.9124	7	222
α	β	γ	Z 1		1.614	27	112	.9097	10	211
Ref. ibid.					1.599	20	201	.8979	7	204
					1.500	4	004	.8961	6	116
ϵ a	n ω β	ϵ γ	Sign		1.452	7	202	.8794	4	212
2V	D _x 7.727 mp	Color			1.366	5	104	.8660	9	215
Ref.					1.276	12	203	.8258	9	313
					1.254	4	210	.8296	5	107
					1.227	14	211	.8215	4	401
SAMPLE FROM JOHNSON, MATTHEY AND CO., LTD. SPECT. ANAL. 1.4% Ca, Si; <0.001% Al, Mg; <0.01% Ag, B, Ba, Fe, Ti; <0.001% Mn, Pb, Sn.					1.1807	8	114	.8070	5	224
X-RAY PATTERN AT 26°C.					1.1566	5	212			
T. P. TO CUBIC FORM BY HEATING 3 HOURS AT 700°C					1.1282	8	105			
					1.1125	3	204			
					1.1058	5	200			

211

6-0601

d	2.22	1.84	3.08	5.57	Nd(OH) ₃					
I/I ₁	100	100	85	80	NEODYMIUM HYDROXIDE					
Rad. CuKα	λ	1.5405	Filter Ni		d Å	I/I ₁	hkl	d Å	I/I ₁	hkl
Dia. Cut off			Coll.		5.57	80	100			
I/I ₁ SPECTROMETER			d corr. sba?		3.20	65	110			
Ref. ROY AND MCKINSTRY, ACTA CRYST. 2, 366 (1953)					3.08	85	101			
Sys. HEXAGONAL			S.G. C _{6h} - P6 ₃ /u		2.768	10	200			
a ₀ 6.421 b ₀	c ₀ 3.74	A	C		2.45	5	111			
α β γ		Z			2.217	100	201			
Ref. ibid.					2.092	10	210			
					1.948	50	300			
					1.842	100	211			
					1.605	30	220			
δ α		n ω β	f γ	Sign	1.540	10	310			
2V	D	mp	Color		1.417	20	311			
Ref.					1.392	10	400			
					1.311	15	401			
					1.290	10	410			

456

5-0584 MINOR CORRECTION

d	3.04	2.64	1.86	4.304	Tl ₂ O ₃					
I/I ₁	100	42	33	11	THALLIUM (III) OXIDE					
Rad. CuKα ₁	λ	1.5405	Filter Ni		d Å	I/I ₁	hkl	d Å	I/I ₁	hkl
Dia. Cut off			Coll.		4.304	11	211	1.462	1	640
I/I ₁ D. C. DIFFRACTOMETER			d corr. sba?		3.042	100	222	1.434	3	721
Ref. SWANSON AND FUYAT, NBS CIRCULAR 539, VOL. II, 28 (1953)					2.816	3	321	1.409	2	642
Sys. CUBIC			S.G. T _h - I ₂ 3		2.635	42	400	1.339	3	732
a ₀ 10.543 b ₀	c ₀	A	C		2.484	6	411	1.318	3	800
α β γ		Z, 16			2.357	2	420	1.298	4	811
Ref. ibid.					2.248	4	332	1.279	2	820
					2.149	1	422	1.2597	2	653
					2.068	8	510	1.2428	1	822
δ α		n ω β	f γ	Sign	1.924	3	521	1.2261	3	831
2V	D _h 10.916 mp		Color		1.863	33	440	1.2094	6	662
Ref.					1.808	2	530	1.1789	4	840
					1.758	1	600	1.1646	1	910
					1.710	5	611	1.1371	2	921
					1.668	2	620	1.1110	1	930
					1.628	4	541	1.0874	1	932
					1.589	27	622	1.0764	2	844
					1.554	6	631	1.0649	1	941
					1.522	6	444			
					1.491	3	710			

1970

5-0602 MINOR CORRECTION

d	2.98	1.97	2.28	3.41	La ₂ O ₃					
I/I ₁	100	63	58	34	LANTHANUM OXIDE					
Rad. CuKα ₁	λ	1.5405	Filter Ni		d Å	I/I ₁	hkl	d Å	I/I ₁	hkl
Dia. Cut off			Coll.		3.41	34	100	1.0901	7	213
I/I ₁ G. C. DIFFRACTOMETER			d corr. sba?		3.063	31	002	1.0658	4	302
Ref. SWANSON AND FUYAT, NBS CIRCULAR 539, VOL. III, 135 (1953)					2.980	100	101	1.0220	<1	006
Sys. HEXAGONAL			S.G. D _{3h} - P321		2.278	58	102	0.9952	3	205
a ₀ 3.9373 b ₀	c ₀ 6.1299	A	C 1.557		1.968	63	110	.9840	3	220
α β γ		Z 1			1.753	52	103	.9787	1	106
Ref. ibid.					1.705	4	200	.9459	<1	310
					1.656	24	112	.9372	3	222
					1.642	17	201	.9345	5	311
δ α		n ω β	f γ	Sign	1.532	3	004	.9131	2	304
2V	D _h 6.573 mp		Color		1.490	5	202	.9070	2	116
Ref.					1.398	2	104	.8883	5	215
					1.309	7	203	.8766	1	206
					1.289	2	210	.8583	4	313
					1.261	12	211	.8480	2	107
					1.209	6	114	.8443	1	401
					1.1879	4	212	.8283	2	224
					1.1538	4	105	.8050	1	314
					1.1396	2	204	.8007	2	117, 216
					1.1367	4	300			

1982

Barium Copper Yttrium Oxide, $\text{Ba}_2\text{Cu}_3\text{YO}_7$

Sample

The sample was obtained from F. Beech of the Reactor Radiation Division, NBS. A stoichiometric mixture of CuO , Y_2O_3 and BaCO_3 was intimately mixed and fired at 500°C overnight. Reaction with container was avoided by placing the pellet on a support of the same material. The resulting powder was ground and pressed into pellets and re-fired at 900°C overnight. The pellets were reground, repressed, and fired at 950°C overnight. Final annealing took place at 750°C for 27 hours under oxygen.

Color

Black

Symmetry classifications

Crystal system Orthorhombic
Space group $\text{Pmmn} (47)$
Pearson symbol $\text{oP}13$
Structure type Distorted perovskite

Data collection and analysis parameters

Radiation $\text{CuK}\alpha_1$
Scanned to $5^\circ 2\theta$
Wavelength 1.5405981 \AA
Mean temperature 25.5°C
 2θ standards Silicon, FP

Crystallographic constants

$a = 3.8856 (3) \text{ \AA}$
 $b = 11.6804 (7)$
 $c = 3.8185 (4)$

$a/b = 0.3327$
 $c/b = 0.3269$

$V = 173.30 \text{ \AA}^3$

$Z = 1$

Density (calc.) = 6.383 g/cm^3

Figures of merit

$F_{30} = 66 (0.0091, 50)$
 $M_{20} = 71$

Comments

The structure was determined by T. Siegrist and S. Sunshine *et al.*¹. The sample was characterized by neutron Rietveld refinement technique by A. Santoro at NBS. Superconductor with T_c of 92K . The compound was first reported by Cava and Batlogg².

References

1. Siegrist, T. *et al.* (1987). Phys. Rev. Lett., to be published.
2. Cava, R. *et al.* (1987). Phys. Rev. Lett., to be published.

$d(\text{\AA})$	$ F^o $	h	k	l	$2\theta (^\circ)$
11.69	1L	0	1	0	7.557
5.836	4	0	2	0	15.169
3.891	10	0	3	0+	22.835
3.819	4	0	0	1	23.274
3.235	3	1	2	0	27.554

(continued)

Barium Copper Yttrium Oxide, $\text{Ba}_2\text{Cu}_3\text{YO}_7$ (continued)

$d(\text{\AA})$	$ F^o $	h	k	l	$2\theta (^\circ)$
3.196	5	0	2	1	27.893
2.918	1L	0	4	0	30.618
2.750	55	1	3	0	32.538
2.725	100	1	0	1+	32.842
2.653	2	1	1	1	33.757
2.468	3	1	2	1	36.370
2.336	13	0	5	0+	38.512
2.319	5	0	4	1	38.799
2.2317	14	1	3	1	40.384
1.9909	2	1	4	1+	45.524
1.9461	22	0	6	0	46.633
1.9425	21	2	0	0	46.725
1.9006	12	0	0	2	47.580
1.7732	4	1	5	1	51.495
1.7406	3	1	6	0	52.526
1.7345	4	0	6	1	52.733
1.7144	2	0	3	2+	53.400
1.6623	2	0	7	0	54.997
1.6595	1	2	2	1	55.313
1.5837	26	1	6	1	58.207

$d(\text{\AA})$	$ F^o $	h	k	l	$2\theta (^\circ)$
1.5685	13	1	3	2	58.826
1.5334	1L	1	7	0	60.309
1.5292	1	0	7	1	60.494
1.4939	2	2	5	0	62.080
1.4899	2	2	4	1	62.262
1.4783	3	0	5	2+	62.809
1.4225	2	1	7	1	65.571
1.3751	5	2	6	0	68.134
1.3666	5	1	8	0	68.618
1.3635	13	0	8	1+	68.797
1.3619	12	2	0	2	68.888
1.2978	1	0	9	0	72.820
1.2951	1L	3	0	0	72.995
1.2865	2	1	6	2+	73.561
1.2657	1L	2	7	0+	74.977
1.2566	1	0	7	2	75.615
1.2341	1L	2	4	2	77.247
1.2309	4	1	9	0	77.480
1.2286	6	0	9	1+	77.654
1.2263	5	3	0	1	77.827

$d(\text{\AA})$	$ F^o $	h	k	l	$2\theta (^\circ)$
1.2099	5	0	3	3+	79.088
1.2015	3	2	7	1	79.749
1.1844	1	1	2	3	81.141
1.1763	2	2	5	2	81.812
1.1702	1L	3	3	1	82.335
1.1683	1	0	10	0	82.498
1.1551	1	1	3	3	83.650
1.1188	3	1	10	0	87.028
1.1161	6	2	8	1+	87.287
1.1114	4	1	8	2	87.748
1.0861	1	3	5	1	90.351
1.0792	1	2	9	0	91.089
1.0734	1	0	9	2+	91.722
1.0617	1	0	11	0	93.027
1.0551	1	2	7	2	93.786
1.0377	4	3	6	1	95.853
1.0333	4	3	3	2	96.394
1.0273	4	1	6	3	97.145

From: Powder Diffraction, Vol.2, No.3, 192-193(1987).

Barium Copper Yttrium Oxide, $\text{Ba}_2\text{Cu}_3\text{YO}_6$

Sample

The sample was obtained from F. Beech of the Reactor Radiation Division, NBS, USA. A stoichiometric mixture of CuO , Y_2O_3 , and BaCO_3 was intimately mixed and fired at 500°C overnight. Reaction with container was avoided by placing the pellet on a support of the same material. The resulting powder was ground and pressed into pellets and refired at 900°C and at 950°C . Final annealing took place at 800°C for 1 hour under argon.

Color

Black

Symmetry classifications

Crystal system Tetragonal
Space group $P4/\text{mmm}$ (123)
Pearson symbol $tP12$

Data collection and analysis parameters

Radiation $\text{CuK}\alpha_1$
Scanned to $5^\circ 2\theta$
Wavelength 1.5405981 \AA
Mean temperature 26.7°C
 2θ Standards Silicon, FP

Crystallographic constants

$a = 3.5878(2) \text{ \AA}$
 $c = 11.8391(7)$
 $c/a = 3.0689$
 $V = 176.20 \text{ \AA}^3$
 $Z = 1$
Density (calc.) = 6.128 g/cm^3

Figures of merit

$F_{30} = 131$ (0.0063,36)
 $M_{20} = 124$

Comments

The structure was determined by neutron Rietveld refinement technique by A. Santoro, et al. (1). The reduced form of high T_c superconductor $\text{Ba}_2\text{Cu}_3\text{YO}_{7-x}$. It is not a superconductor material.

Reference

1. Santoro, A., Miraglia, S., Beech, F., Sunshine, S. A. and Murphy, D. W., (1987). *Mat. Res. Bull.*, 22, 1007.

d	l	h	k	l	2θ
11.85	3	0	0	1	7.453
5.922	5	0	0	2	14.947
3.947	6	0	0	3	22.507
3.860	10	1	0	0	23.022
3.232	15	1	0	2	27.574
2.759	100	1	0	3	32.429
2.729	52	1	1	0	32.793
2.658	1	1	1	1	33.646
2.478	3	1	1	2	36.216
2.3690	9	0	0	5	37.951
2.3484	16	1	0	4	38.296
2.2441	13	1	1	3	40.151
2.0180	2	1	0	5	44.879
2.0066	5	1	1	4	45.148
1.9731	5	0	0	6	45.959
1.9295	34	2	0	0	47.059
1.8338	1	2	0	2	49.677
1.7881	6	1	1	5	51.036
1.7566	1	1	0	6	52.019
1.7330	2	2	0	3	52.782
1.7252	3	2	1	0	53.039
1.6915	3	0	0	7	54.181
1.6565	5	2	1	2	55.422
1.5988	8	1	1	6	57.607
1.5808	26	2	1	3	58.326
1.5486	4	1	0	7	59.659
1.4954	5	2	0	5	62.012
1.4906	8	2	1	4	62.231
1.4375	3	1	1	7	64.805
1.3944	1L	2	1	5	67.064

Barium Copper Yttrium Oxide, $\text{Ba}_2\text{Cu}_3\text{YO}_6$ (continued)

d	l	h	k	l	2θ
1.3820	5	1	0	8	67.752
1.3788	9	2	0	6	67.929
1.3638	8	2	2	0	68.779
1.2986	2	2	1	6	72.769
1.2891	2	2	2	3	73.387
1.2862	1	3	0	0	73.584
1.2718	4	2	0	7	74.556
1.2566	1L	3	0	2	75.611
1.2230	6	3	0	3	78.075
1.2198	10	3	1	0	78.324

d	l	h	k	l	2θ
1.2074	3	2	1	7	79.282
1.1948	1	3	1	2	80.284
1.1841	1	0	0	10	81.167
1.1819	4	2	2	5	81.349
1.1794	3	3	0	4	81.555
1.1654	2	3	1	3	82.746
1.1317	6	1	0	10	85.794
1.1279	3	3	1	4	86.153
1.1234	4	2	1	8	86.575
1.0868	2	2	0	9	90.270

d	l	h	k	l	2θ
1.0843	4	3	1	5	90.531
1.0700	1L	3	2	0	92.091
1.0618	2	2	2	7	93.012
1.0530	1	3	2	2	94.033
1.0375	4	3	1	6	95.883
1.0328	5	3	2	3	96.467
1.0237	1L	3	0	7	97.615
1.0090	2	2	0	10	99.536
1.0062	3	3	2	4	99.908

From: Powder Diffraction, Vol.2, No.2, 114-115(1988).

XRD Integrated Intensities of Ba_2BiYO_6 compound

hkl	I_{cal}	I_{obs}	$\sigma(I_{\text{obs}})$
111	25.6	26.5	1.0
200	4.93	7.54	1.0
220	276.0	274.0	1.4
113	15.8	16.8	0.9
400	79.6	81.5	1.0
331	7.28	5.48	0.9
224	116.0	123.0	1.1
333/115	5.59	5.67	0.9
440	50.5	52.5	1.0
135	5.45	5.41	0.9
620	51.6	52.1	1.0
444	17.0	15.9	0.9
246	63.8	63.2	1.0
$R_I = 2.9\%$			

Structural Parameters for Ba_2BiYO_6

Atom	x/a	y/b	z/c	$B(\text{\AA}^2)$	N^*
Ba	1/4	1/4	1/4	0.3(2.3)	8
Bi	0	0	0	-0.2(1.3)	4
Y	1/2	1/2	1/2	-1.1(2.9)	4
O	0	0	1/4	1.0	24

Space Group $\text{Fm}\bar{3}\text{m}$, $a=8.5675(6)$ Å* N is the occupation per unit cell

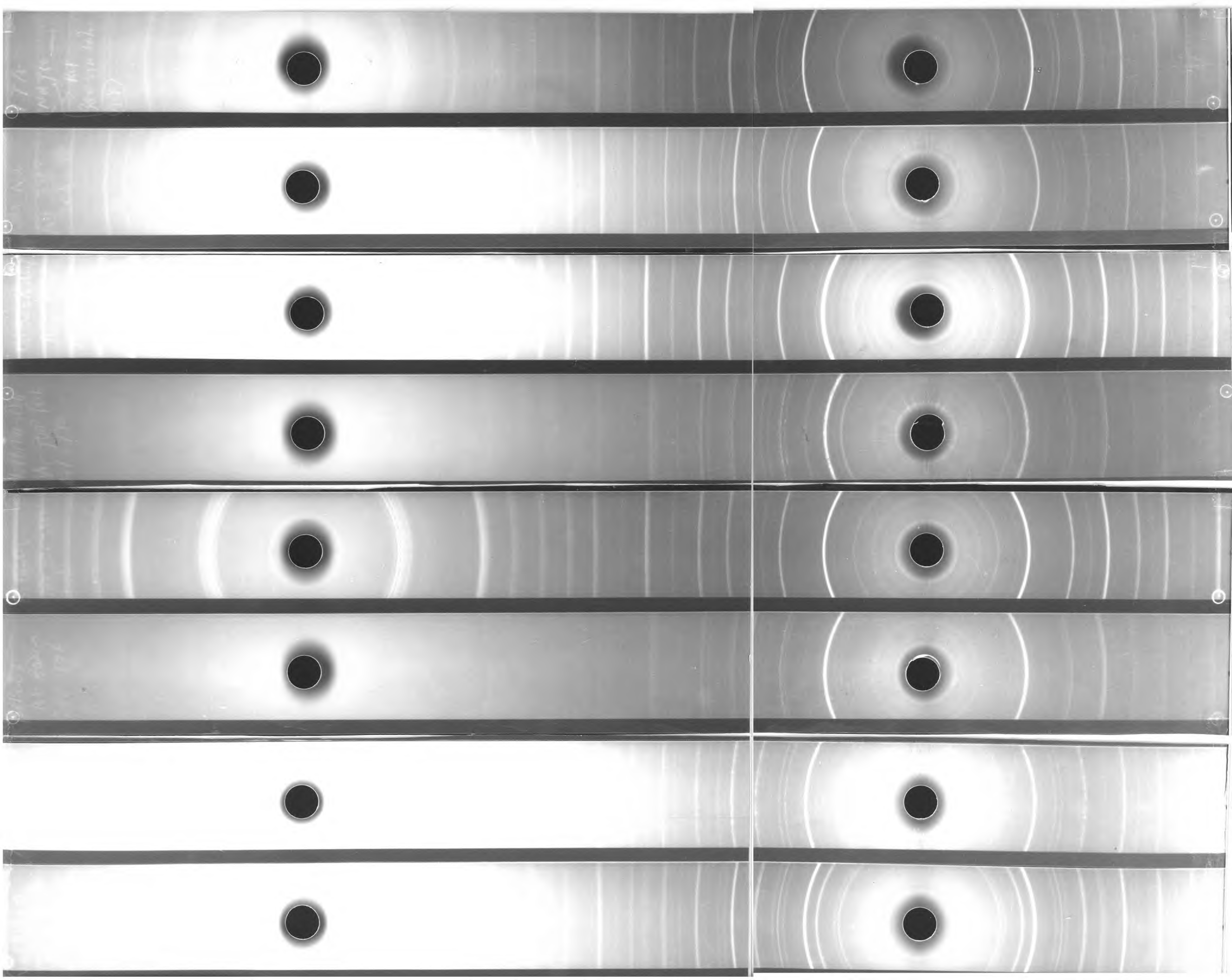
Both from Ref.65.

30-123	30-123	30-123	30-123	30-123	30-123	30-123	30-123	Quality:	
BaCuO ₂									
Barium Copper Oxide									
Rad: CoK α GA Lambda: 1.7902 Filter: d-sp:									
Cutoff: Int: I/I ₀ :									
Migeon, H. et al., \ITRev. Chim. Miner.\RG, \BF13\RG 440 (1976)									
Sys: Cubic S.G.: I432 (211)									
a: 18.282 b: c: A: C:									
A: B: C: Z: mp:									
Ibid.									
Ox: Om: SS/FGM: F#3#0=13.5(0.052,43)									
ea: nwB: ey: Sign: 2V:									
\BFColor\RG Dark brown I									
Made by reaction in air of CuO and BaO at 800 C followed by									
treatment at 100-22 torr at 800 C. Other possible space groups are									
Im3m (229) or I43m (217). Cell parameters generated by least									
squares refinement. Reference reports a=18.26.									
\BAPlus 4 reflections to 1.456									
From JCPDS, 1987.									

From JCPDS, 1987.

APPENDIX II**1. The photographs of some x-ray powder diffraction patterns (from top to bottom of the next page)**

- 1 Orthorhombic Nd-123;
- 2 Tetragonal Nd-123;
- 3 $\text{Ba}_2\text{BiNdO}_6$ made in air;
- 4 $\text{Ba}_2\text{BiNdO}_x$ made in N_2 ;
- 5 BaBiO_3 made in air;
- 6 BaBiO_x made in N_2 ;
- 7 Nominal $\text{Nd}_{0.8}\text{Bi}_{0.2}\text{Ba}_2\text{Cu}_3\text{O}_y$ made in N_2 ;
- 8 Nominal $\text{Nd}_{0.8}\text{Bi}_{0.2}\text{Ba}_2\text{Cu}_3\text{O}_y$ made in N_2 and then annealed in air at 400°C for 20 hours.



2. The X-ray Diffraction Pattern of $\text{Ba}_2\text{BiNdO}_6$

d	hkl	I _{obs}
4.98	111	very very weak
4.35	200	very weak
3.08	220	very strong
2.62	113	very weak
2.17	400	medium
1.95	331	very very weak
1.78	224	strong
1.67	333/115	very very weak
1.538	440	weak
1.454	135	very very weak
1.376	620	medium
1.257	444	very weak
1.163	246	medium

Structure Parameters for $\text{Ba}_2\text{BiNdO}_6$:

Space Group $\text{Fm}\bar{3}\text{m}$, $a = 8.703$.